Earthq Eng & Eng Vib (2022) 21: 947-967 **DOI**: https://doi.org/10.1007/s11803-022-2129-9

A new approach for free vibration analysis of a system of elastically interconnected similar rectangular plates

E. Heidari† and A. Ariaei‡

Department of Mechanical Engineering, Faculty of Engineering, University of Isfahan, Isfahan 8174673441, Iran

Abstract: A new procedure is proposed to ease the analyses of the free vibration of an elastically connected identical plates system with respect to Kirchhoff plate theory. A structure of *n* parallel, elastically connected rectangular plates is of concern, whereby the motion is explained by a set of *n* coupled partial differential equations. The method involves a new change in variables to uncouple equations and form an equal system of *n* decoupled plates, while each is assumed to be elastically connected to the ground. The differential quadrature method is adopted to solve the decoupled equations. To unravel the original system, the inverse transform is applied. Decoupling the equations enables one to solve them based on the solution methods available for a single plate system. This also diminishes the computational costs of such problems. By considering different boundary conditions, a case study is run to present the method and to validate the results with its counterparts, for which excellent agreement is observed. Assessing the influence of dimensionless thickness, aspect ratio, and stiffness coefficients on the frequencies reveals the different effects of them at the low order of dimensionless natural frequencies in comparison with high orders and for different boundary conditions.

Keywords: multiple-plate system; elastic connections; free vibration; Kirchhoff plate theory; differential quadrature method

1 Introduction

Consisting of different continuous systems, coupled structures are highly applied in engineering fields; consequently, there exist many studies concerning them in the field of mechanical behavior. The complexity of coupled structures centers on their feature of having continuous components. Coupled structures consisting of beams are one of these systems which have received much attention during these years (Del Carpio *et al*., 2017; Jouneghani and Haghollahi, 2020; Ketiyot and Hansapinyo, 2018; Li *et al*., 2020; Liu *et al*., 2020). Many studies of this category have been done on the elastically connected double and multiple beam systems. The interaction between external moving loads and multiple beams systems is the subject of a study run by Foroozandeh and Ariaei (2018). By applying the Timoshenko beam theory, they assessed the effects of inertia and different types of acceleration on system response. There are similar studies in which this issue is assessed (Ariaei *et al*., 2011; Paunović *et al*., 2020; Feng *et al*., 2020). Brito *et al*. (2019) applied the boundary element method (BEM) to analyze a double beam system, in which the Winkler foundation theory is compared with that of Pasternak. Liu and Yang (2019) and Zhao *et al*. (2020) provided a closed-form solution for the free and forced vibration of double beam systems, in which the main feature is applying Green′s functions.

Double and multiple plate systems are other types of complicated coupled structures, which have many applications. In absorbing the vibration of large deck plates of ships, bridges, optical tables, computer disk drives, hard drives, multi-array drives of computer servers, and general tooling machines, the double plate systems are highly contributive and feasible. Next to the practical problems in construction and the complexities in solving the equations as limitations, there also are advantages in designing lightweight structures that represent excellent practical fields in structural engineering, such as in aeronautical and mechanical engineering. Double and multiple plate systems are observed in the aerospace industry, for example, space platforms, solar panels, and the skin of planes′ wings (Giles, 1995). In civil engineering, solutions obtained from theoretical approaches of this type of structure can be applied for estimating the behavior of multi-story buildings (Stojanović *et al*., 2015). Arthi and Jaya (2020) studied the seismic performance of a double concrete plate system consisting of a shear wall and a slab to provide a seismic resistant connection for precast elements used

Correspondence to: Alireza Ariaei, Department of Mechanical Engineering, Faculty of Engineering, University of Isfahan, Isfahan 8174673441, Iran
Tel: +98-3137934054; Fax: +98-3137932746
E-mail: ariaei@eng.ui.ac.ir
†PhD Candidate; ‡Assistant Professor

Supported by: Iran National Science Foundation (INSF) under Grant No. 97021731
Received November 14, 2020; **Accepted** April 11, 2022

in the structure. Multi-plate systems can be applied to reduce the seismic effect on various structures. Li and Shu (2020) applied Triangular-plate added damping and stiffness (TADAS) device which is a multiple triangular plate system. Maleki and Dolati (2020) applied the multi-plate system as the end diaphragm in the tub girder of bridges to reduce seismic demand by more than 25%. Multiple plate systems can also be used to simulate the dynamic behavior of multilayer soils (Chao *et al*., 2020; Li *et al*., 2018), wherein the multi-degree of freedom (MDOF) analysis method can be applied to simplify the solution. Applying powerful methods such as Rayleigh_ Ritz, finite element, transfer matrix, etc., for solving complex geometries is feasible. However, simplifying complex structures by the inclusion of coupled identified structures such as plates, beams, etc., in reducing the calculation effort has been assessed by some researchers. One of the most well-known structures of this type is laminated composite materials that may be modeled as a structure consisting of several plates connected by elastic or viscoelastic soft material. In case intermediate layers have negligible mass and a shear modulus; one can only take into account their compressibility and model this type of laminate by applying the method proposed in this article. This leads to having only normal stress, with no need to fulfill the continuity conditions in the shear strains in various layers′ interfaces, which results in a simplification of equations and the computational process. A high strength and stiffness-to-weight ratio of laminated composite materials provide major reasons for applying them in a wide variety of mechanical and civil engineering systems such as the aircraft, automobile, train, and construction industries. As to energy harvesters, inserting piezoelectric layers in such combinations has become intriguing in scientific community harvesters (Yuan *et al*., 2017; Khazaee *et al*., 2020; Fu *et al*., 2020; Tian *et al*., 2020; Liu *et al*., 2020).

The concept of the coupled plate systems field was applied by McElman (1964), who assessed the flutter of a simply supported double plate system, subject to a combination of mid-plane loads and aerodynamic pressure by assuming a quasi-static condition (high Mach number) and not considering the damping term. McElman also drew some sketches, illustrating system buckling behavior. In a similar study, Bismark-Nasr (1977) applied the FE method to explain the stability features of the same system, in which the damping term of aerodynamic pressure was of concern. By adopting the Winkler foundation theory, Kunukkasseril and Swamidas (1973) and Swamidas and Kunukkasseril (1975, 1978) assessed the free vibrations of elastically connected circular plate systems. Kunukkasseril and Swamidas (1975) also introduced an analytical solution for the stability of circular double plate systems with different boundary conditions. The Kirchhoff plate theory was applied by Chonan (1976, 1979a) to assess the free vibration of elastically connected multiple circular and annular plate systems subjected to elastic boundary conditions, by which an attempt was made to classify the mode shapes and consider the effect of in-plane loads on natural frequencies. In other studies carried out by Chonan (1979b, 1979c), the Kelvin model was applied to analyze the stability of double Mindlin rectangular plates connected by a viscoelastic medium subject to a moving load. With reference to internal material damping and based on Mindlin plate theory, the forced vibration of an annular double plate system with different boundary conditions was assessed by Irie *et al*. (1982). A method based on Green′s functions was proposed by Kukla (1998, 1999) to solve the free vibration of a system consisting of two plates connected by a continuous and discontinuous Winkler medium; it was revealed that the elastic connection size affects system frequencies. By applying the classical Navier method, the natural frequencies of an elastically connected double plate system were determined by Oniszczuk (2000) and a comparison was made with a double membrane system to establish their similarity. This study was extended by Oniszczuk (2004) to embody forced vibration and to illustrate that the second plate can behave as a dynamic vibration absorber. Applying the double plate configuration in absorbing and reducing vibration has been of significant concern in many studies (Aida *et al*., 1995; Wang and Chen, 2013; Wang and Lin, 2016; Kamenskikh and Lekomtsev, 2020). Hedrih (2006, 2007, 2008) and Hedrih and Simonović (2012) assessed the free and forced vibration of rectangular and circular double plate systems by applying Kelvin foundation theory subject to discontinuity in the elastic medium, nonlinearity, and different boundary conditions assumptions. The effect of connecting rolling viscous nonlinear elastic elements on the forced vibration of a double plate system was assessed by Simonović (2012), whereby it was revealed that rolling elements inertia intensified resonant transition phenomena. The intersection between a double plate system and soil (as a connecting medium) by applying the Winkler and Pasternak foundation theory was modeled by Rosa and Lippiello (2009) to analyze the free vibration of the system subject to simply supported boundary conditions. The coupled plate systems are applicable in the fuel assembly of reactors and heat exchangers, and their oscillating behavior was studied (Jeong, 2006; Jeong and Kim, 2009; Jeong and Kang, 2013; Bochkarev and Lekomtsev, 2016). Ma *et al*. (2014) proposed an active triple-panel sound insulation system with a controllable force acting on the middle plate. An analytical method was adopted by Sadri and Younesian (2016) in assessing the vibrational and acoustic responses of a sandwich plate coupled with an enclosure cavity, by which it was assumed that the resilient material between the layers was of a Winkler medium and it was found that cavity thickness had a reverse effect on plate frequencies. The connecting resilient material effect on the stability behavior of a cross-ply laminated plate was studied by Stojanović *et al*. (2019), whereby the viscoelastic

assumption was applied for the connecting material. Stojanović *et al*. (2015) assessed the vibrational and stability behavior of multiple plate systems by applying the Winkler foundation theory. When the thickness of the plate is small compared to its other dimensions, the Kirchhoff plate theory is applied, whereby the effects of rotary inertia and shear deformation are ignored. For thick plates, however, the Mindlin plate theory was applied (Rao, 2007). Although, when considering thin plates, the Kirchhoff plate theory is of concern in this article; nonetheless, the proposed method can be extended to higher-order plate theories such as that of Mindlin.

Because exact solution methods are not always available, approximate numerical methods (Abdel Raheem *et al*., 2018; Bendine *et al*., 2016; Dusicka *et al*., 2004; Gu *et al*., 2018; Liu *et al*., 2016; Lu *et al*., 2004; Tahouneh *et al*., 2019, 2020; Wu and Zhong, 2003) are preferred. However, due to the accuracy and the convenience of doing parametric studies, applying analytical and semi-analytical solutions (Busby and Weingarten, 1972; Ebrahimi and Heidari, 2019; Lobitz *et al*., 1977; Nayfeh *et al*., 1974; Bayat and Pakar, 2013; Wang, 2018; Wang *et al*., 2020; Wang *et al*., 2019; Wang and Zhao, 2019; Wang and Zu, 2017a, 2017b; Yang and Wang, 2020) are more appropriate. By applying an analytical procedure, a new approach is proposed to uncouple the governing equations of multiple-plate systems to enable one to solve them based on the solution methods available for a single plate system; thus, there is a reduction in the computational costs of such coupled problems.

In the referenced articles for coupled beam and plate systems, a double-plate system connected by an elastic layer, a multiple-plate system in a sandwich structure, or a system of elastically connected beams are often studied. Simultaneously solving the governing equations of coupled plate systems is essential, wherein calculations are time consuming, especially when the number of plates increases. By considering *n* elastically, interconnected rectangular plates, a new method involving a change in variables is proposed to uncouple a set of *n* partial differential equations into independent ones and to extend the work done by Ghafarian and Ariaei (2016), wherein a multiple beams system is of concern. This leads to converting and reducing the solution of elastically interconnected plates to the solution of independent plates with a slight computational effort, which is especially evident for many plates. Another additional feature is the second moment of mass, which is absent in some references for thin plates. The necessity of identical plates and identical boundary conditions on the same side is the only restricting assumption for this method.

This article is organized as follows: the problem formulation is introduced in Sec. 2; results and discussions are presented in Sec. 3, and the conclusion appears in Sec. 4. To represent this technique in detail a case study with three plates is discussed in Sec. 3; frequencies and mode shapes are acquired; and several parameters′ effects, such as dimensionless thickness, aspect ratio, and layers stiffness coefficients, are listed in several tables and figures.

2 Problem formulation

2.1 Differential equations of motion

A system of *n* elastically connected, rectangular Kirchhoff plates, joined continuously by elastic layers, is assumed, as shown in Fig. 1. The length, width, and thickness of each plate are *a*, *b* and *h*, respectively. Without affecting the solution approach, all plates of the system are assumed to be clamped on one side and free on the other (the C-F-F-F boundary condition). The Winkler layer has the linear stiffness coefficients of *k*, the displacements are minor, and the material is homogeneous and isotropic.

Based on Kirchhoff plate theory, the strain-displacement equations, constitutive equations, and Hamilton principle (Reddy, 2006), the vibration equation for one plate is expressed as:

$$\begin{aligned} &D\left(w_{i,xxxx}+2w_{i,xxyy}+w_{i,yyyy}\right)+k_i\left(w_i-w_{i-1}\right)+\\ &k_{i+1}\left(w_i-w_{i+1}\right)=-I_0\ddot{w}+I_2\left(\ddot{w}_{i,xx}+\ddot{w}_{i,yy}\right)\\ &i=1,\ 2,\ \ldots,\ n \end{aligned} \tag{1}$$

where, w_i is the transverse deflection of *i*th plate, k_i is the stiffness of the elastic medium between the (*i*-1)th and *i*th plate, $I_0=\rho h$ is the mass density per unit area of the plate surface (the zero-th moment of mass), and $I_2=\rho h^3/12$ is the second moment of mass.

The parameter *D* is defined as:

$$D=\frac{Eh^3}{12\left(1-\upsilon^2\right)} \tag{2}$$

where, ρ, E and υ are the density, Young′s modulus, and the Poisson′s ratio, respectively. To apply these to the first and last plate, w_0, w_{n+1}, and k_{n+1} values are set to be zero in Eq. (1).

The boundary condition of the *i*th plate is expressed as (Reddy, 2006):

$x = 0$ (clamped)

$$w_i=0 \quad \frac{\partial w_i}{\partial x}=0 \tag{3}$$

$x = a$ (Free)

$$w_{i,xx}+\upsilon w_{i,yy}=0 \quad w_{i,xxx}+\left(2-\upsilon\right)w_{i,xyy}=0 \tag{4}$$

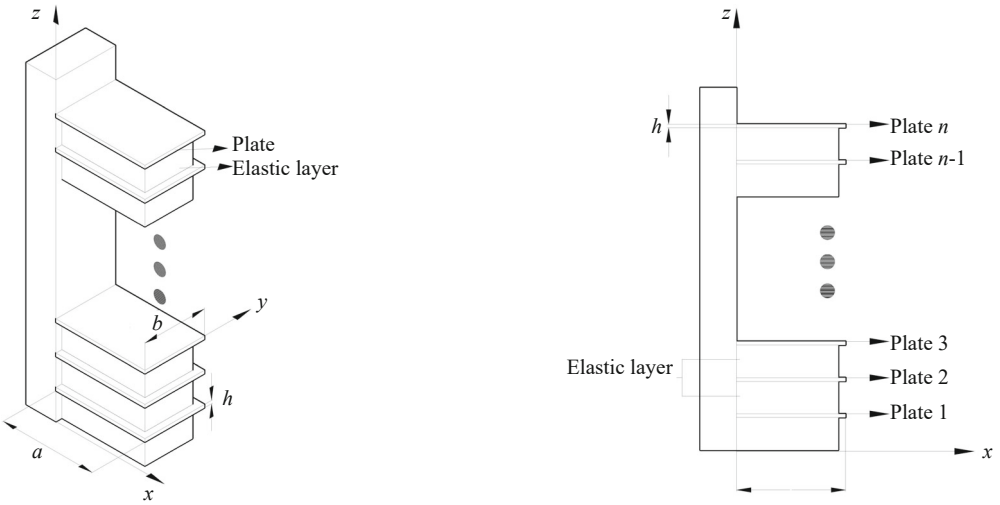

Fig. 1 Schematic of a system of n elastically connected rectangular plates

$y = 0$, b (Free)

$$w_{i,yy} + \upsilon w_{i,xx} = 0 \quad w_{i,yyy} + (2-\upsilon) w_{i,yxx} = 0 \tag{5}$$

At the corner of the two adjacent free edges, the following equation is applied for the boundary condition (Reddy, 2006; Shu, 2012):

$$w_{i,xy} = 0 \tag{6}$$

2.2 Decoupling of the equations of motion

That Eq. (1) forms a system of n coupled, partial differential equations that are not easily solvable is evident. Through a correct manipulation of the variables the equations of motion are uncoupled, which would enable solving them separately in a straightforward manner. By reversing the method, the anticipated parameters of the original system, such as the natural frequencies and the mode shapes become extracted. The new variable u_p is defined by (Ariaei *et al*., 2011; Ghafarian and Ariaei, 2016):

$$u_p(x,y,t) = \sum_{i=1}^{n} c_{pi} w_i(x,y,t) \quad p = 1,\ 2,\ ...,\ n \tag{7}$$

where, p is the plates′ count $(p = 1,\ 2,\ \ldots,\ n)$. The coefficients c_{pi} should be identified in a manner as to uncouple the equations. Multiplying the ith equation by coefficient c_{pi} and then adding them would yield:

$$\begin{aligned} &\sum_{i=1}^{n} c_{pi} \left[D\left(w_{i,xxxx} + 2w_{i,xxyy} + w_{i,yyyy}\right) + \right. \\ &\left. k_i\left(w_i - w_{i-1}\right) + k_{i+1}\left(w_i - w_{i+1}\right) \right] = \\ &\sum_{i=1}^{n} c_{pi} \left[-I_0 \ddot{w} + I_2 \left(\ddot{w}_{i,xx} + \ddot{w}_{i,yy} \right) \right] \\ &p = 1,\ 2,\ ...,\ n \end{aligned} \tag{8}$$

By considering Eq. (7), Eq. (8) is rewritten as:

$$\begin{aligned} &D\left(u_{p,xxxx} + 2u_{p,xxyy} + u_{p,yyyy}\right) + \\ &\sum_{i=1}^{n} c_{pi} \left(k_i\left(w_i - w_{i-1}\right) + k_{i+1}\left(w_i - w_{i+1}\right) \right) = \\ &-I_0 \ddot{u}_p + I_2 \left(\ddot{u}_{p,xx} + \ddot{u}_{p,yy} \right) \\ &p = 1,\ 2,\ ...,\ n \end{aligned} \tag{9}$$

In a similar manner, the new equations for boundary conditions Eqs. (3)–(6) are expressed as:

$x = 0$ (clamped)

$$u_p = 0 \quad \frac{\partial u_p}{\partial x} = 0 \tag{10}$$

$x = a$ (Free)

$$u_{p,xx} + \upsilon u_{p,yy} = 0 \quad u_{p,xxx} + (2-\upsilon) u_{p,xyy} = 0 \tag{11}$$

$y = 0, b$ (Free)

$$u_{p,yy} + \upsilon u_{p,xx} = 0 \quad u_{p,yyy} + (2-\upsilon) u_{p,yxx} = 0 \quad (12)$$

and at the free corners:

$$u_{p,xy} = 0 \quad (13)$$

In rewriting the pth equation in Eq. (9), by considering only one function of $u_p(x,y,t)$, a decoupled set of equations would yield, provided that the following equation holds:

$$\sum_{i=1}^{n} c_{pi}\left(k_i\left(w_i - w_{i-1}\right) + k_{i+1}\left(w_i - w_{i+1}\right)\right) = \alpha_p u_p \quad (14)$$

By inserting Eq. (7) in Eq. (14) with some rearrangements, Eq. (15) is arrived at, as follows:

$$\begin{bmatrix} w_1 & w_2 & w_3 & \cdots & w_{n-1} & w_n \end{bmatrix}_{1\times n} \cdot \begin{bmatrix} k_1+k_2 & -k_2 & 0 & \cdots & \cdots & \cdots & 0 \\ -k_2 & k_2+k_3 & -k_3 & \cdots & \cdots & \cdots & 0 \\ 0 & -k_3 & \ddots & \cdots & \cdots & \cdots & 0 \\ \vdots & \vdots & \vdots & \cdots & \cdots & \cdots & \vdots \\ \vdots & \vdots & \vdots & \cdots & \ddots & -k_{n-1} & 0 \\ \vdots & \vdots & \vdots & \cdots & -k_{n-1} & k_{n-1}+k_n & -k_n \\ 0 & 0 & 0 & \cdots & 0 & -k_n & k_n \end{bmatrix}_{n\times n} \cdot \begin{bmatrix} c_{p1} \\ c_{p2} \\ \vdots \\ c_{pn} \end{bmatrix}_{n\times 1} = \alpha_p \begin{bmatrix} w_1 & w_2 & w_3 & \cdots & w_{n-1} & w_n \end{bmatrix}_{1\times n} \begin{bmatrix} c_{p1} \\ c_{p2} \\ \vdots \\ c_{pn} \end{bmatrix}_{n\times 1} \quad (15)$$

As to the independency of the functions of w_i (i = 1, 2, …, n), to satisfy Eq. (15), it is essential to have:

$$\begin{bmatrix} k_1+k_2 & -k_2 & 0 & \cdots & \cdots & \cdots & 0 \\ -k_2 & k_2+k_3 & -k_3 & \cdots & \cdots & \cdots & 0 \\ 0 & -k_3 & \ddots & \cdots & \cdots & \cdots & 0 \\ \vdots & \vdots & \vdots & \cdots & \cdots & \cdots & \vdots \\ \vdots & \vdots & \vdots & \cdots & \ddots & -k_{n-1} & 0 \\ \vdots & \vdots & \vdots & \cdots & -k_{n-1} & k_{n-1}+k_n & -k_n \\ 0 & 0 & 0 & \cdots & 0 & -k_n & k_n \end{bmatrix}_{n\times n} \cdot \begin{bmatrix} c_{p1} \\ c_{p2} \\ \vdots \\ c_{pn} \end{bmatrix}_{n\times 1} = \alpha_p \begin{bmatrix} c_{p1} \\ c_{p2} \\ \vdots \\ c_{pn} \end{bmatrix}_{n\times 1} \quad (16)$$

In matrix notation, Eq. (16) is expressed as:

$$\left(\boldsymbol{K} - \alpha_p \boldsymbol{I}\right)\boldsymbol{c}_p = 0 \quad (17)$$

where, $\boldsymbol{I}$ is the unit matrix and matrices $\boldsymbol{K}$ and $\boldsymbol{c}_p$ are defined through:

$$\boldsymbol{K} = \begin{bmatrix} k_1+k_2 & -k_2 & 0 & \cdots & \cdots & \cdots & 0 \\ -k_2 & k_2+k_3 & -k_3 & \cdots & \cdots & \cdots & 0 \\ 0 & -k_3 & \ddots & \cdots & \cdots & \cdots & 0 \\ \vdots & \vdots & \vdots & \cdots & \cdots & \cdots & \vdots \\ \vdots & \vdots & \vdots & \cdots & \ddots & -k_{n-1} & 0 \\ \vdots & \vdots & \vdots & \cdots & -k_{n-1} & k_{n-1}+k_n & -k_n \\ 0 & 0 & 0 & \cdots & 0 & -k_n & k_n \end{bmatrix}_{n\times n}$$

$$\boldsymbol{c}_p = \begin{bmatrix} c_{p1} \\ c_{p2} \\ \vdots \\ c_{pn} \end{bmatrix}_{n\times 1} \quad (18)$$

Equation (17) is an eigenvalue problem wherein α_p and $\boldsymbol{c}_p$ are the pth eigenvalue and eigenvector of Matrix $\boldsymbol{K}$, respectively. To have a nontrivial solution it is necessary that:

$$\det\left(\boldsymbol{K} - \alpha_p \boldsymbol{I}\right) = 0 \quad (19)$$

The eigenvalues of matrix $\boldsymbol{K}$ obtained through Eq. (19) are applied to extract the corresponding eigenvectors from Eq. (17), the components of which are the coefficients shown in Eq. (7). By applying these eigenvectors in defining the new variable $u_p(x,y,t)$, the equations are uncoupled; that is, the existence of α_p values and $\boldsymbol{c}_p$ vectors assure that Eq. (9) is uncoupled. By applying Eq. (14) in Eq. (9), the new decoupled equations are expressed as:

$$D\left(u_{p,xxxx} + 2u_{p,xxyy} + u_{p,yyyy}\right) + \alpha_p u_p = -I_0 \ddot{u}_p + I_2\left(\ddot{u}_{p,xx} + \ddot{u}_{p,yy}\right) \quad p = 1,\ 2,\ ...,\ n \quad (20)$$

Equation (20) and boundary conditions Eqs. (10)–(13) constitute a new system of n separated plates with no mutual interaction. Figure 2(b) shows a schematic of this new system. Here, the original system consisting of n connected plates is transformed into a system of n decoupled plates, where the pth plate independently appears on a Winkler foundation with the spring coefficient α_p elastically connected to the ground, as shown in Fig. 2. In other words, the decoupled plates

system pictured in Fig. 2(b) is a mathematically obtained system related to Eq. (20), with boundary described in Eqs. (10)–(13). The same method is adopted in solving the uniform Eq. (20). By applying the reverse transformation, the original system's solution is obtained.

2.3 The free vibration problem

To solve Eq. (20), the following harmonic motion is considered as follows:

$$u_p(x,y,t) = U_p(x,y)\mathrm{e}^{\mathrm{i}\omega_p t} \tag{21}$$

where, $U_p(x,y)$ and ω_p are the amplitude and natural frequencies of the pth plate, respectively.

To simplify the formulas, the following dimensionless parameters are introduced:

$$\Omega_p^2 = \frac{I_0 a^4}{D}\omega_p^2,\ X = \frac{x}{a},\ Y = \frac{y}{b},$$
$$\bar{U}_p = \frac{U_p}{h},\quad \lambda = \frac{a}{b},\quad \bar{h} = \frac{h}{a},\quad \bar{\alpha}_p = \frac{a^4}{D}\alpha_p \tag{22}$$

Inserting Eq. (21) into Eq. (20) and applying the dimensionless parameters of Eq. (22), yield:

$$\bar{U}_{p,XXXX} + 2\lambda^2\bar{U}_{p,XXYY} + \lambda^4\bar{U}_{p,YYYY} + \bar{\alpha}_p\bar{U}_p + \Omega_p^2\left[-\bar{U}_p + \frac{\bar{h}^2}{12}\bar{U}_{p,XX} + \lambda^2\frac{\bar{h}^2}{12}\bar{U}_{p,YY}\right] = 0$$
$$p = 1,\ 2,\ \ldots,\ n \tag{23}$$

By applying a similar method for Eqs. (10)–(13), the dimensionless boundary conditions are obtained as:

$X = 0$ (clamped)

$$\bar{U}_p = 0 \quad \frac{\partial\bar{U}_p}{\partial X} = 0 \tag{24}$$

$X = 1$ (Free)

$$\bar{U}_{p,XX} + \nu\lambda^2\bar{U}_{p,YY} = 0 \quad \bar{U}_{p,XXX} + (2-\nu)\lambda^2\bar{U}_{p,XYY} = 0 \tag{25}$$

$Y = 0,1$ (Free)

$$\lambda^2\bar{U}_{p,YY} + \upsilon\bar{U}_{p,XX} = 0 \quad \lambda^2\bar{U}_{p,YYY} + (2-\nu)\bar{U}_{p,YXX} = 0 \tag{26}$$

Free corners

$$\bar{U}_{p,XY} = 0 \tag{27}$$

The solution of Eq. (23) by considering boundary conditions Eqs. (24)–(27) leads to obtaining the frequencies and modes of the pth plate in the decoupled plates system. Each natural frequency in the decoupled plates system is one of those found in the original system. By back-substituting them in Eq. (21) and then using that result into Eq. (7), the original system′s modes are found. Equation (7) is rewritten in a matrix notation as:

$$\boldsymbol{U} = \boldsymbol{CW} \tag{28}$$

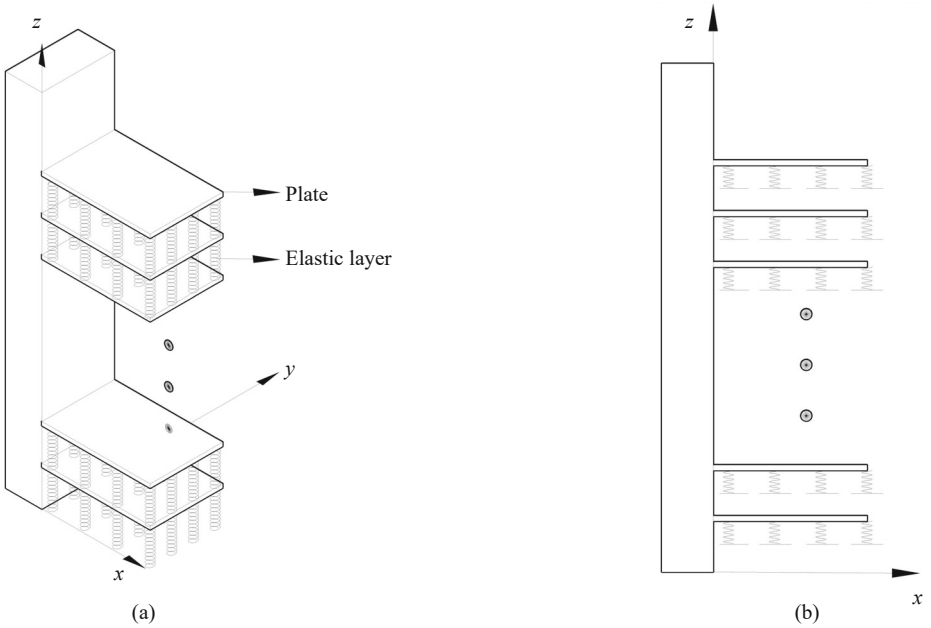

Fig. 2 The transformation from the coupled plate system to the decoupled plate system. (a) Coupled plate system, (b) decoupled plate system

where,

$$\boldsymbol{U}=\begin{bmatrix}u_1 & u_2 & \cdots & u_n\end{bmatrix}^{\mathrm{T}} \quad \boldsymbol{W}=\begin{bmatrix}w_1 & w_2 & \cdots & w_n\end{bmatrix}^{\mathrm{T}}$$
$$\boldsymbol{C}=\begin{bmatrix}c_{11} & c_{12} & \cdots & c_{1n}\\ c_{21} & \cdots & \cdots & c_{2n}\\ \vdots & \vdots & \vdots & \vdots\\ c_{n1} & c_{n2} & \cdots & c_{nn}\end{bmatrix} \tag{29}$$

Possessing the variable $u_p(x,y,t)$, the original system's variables $w_i(x,y,t)$ are calculated through the use of the following equation:

$$\boldsymbol{W}=\bar{\boldsymbol{C}}\boldsymbol{U} \tag{30}$$

where,

$$\bar{\boldsymbol{C}}=\begin{bmatrix}\bar{c}_{11} & \bar{c}_{12} & \cdots & \bar{c}_{1n}\\ \bar{c}_{21} & \cdots & \cdots & \bar{c}_{2n}\\ \vdots & \vdots & \vdots & \vdots\\ \bar{c}_{n1} & \bar{c}_{n2} & \cdots & \bar{c}_{nn}\end{bmatrix}=\boldsymbol{C}^{-1} \tag{31}$$

Because the rows of matrix $\boldsymbol{C}$ are the eigenvectors of the symmetric matrix $\boldsymbol{K}$ and are linear independent, matrix $\boldsymbol{C}$ is invertible.

By applying Eq. (30), the vector $\boldsymbol{W}$ of the original system is obtained from the vector $\boldsymbol{U}$ of the decoupled plate system. As the pth plate of the decoupled plate system becomes oscillated at its jth natural frequency and mode shape $\left(\text{i.e.},U_{pj}(x,y),\omega_{pj}\right)$, Eqs. (21) and (30) reveal that all plates of the original system vibrate at the same frequency, ω_{pj}, which is the natural frequency of the original system, displayed in Fig. 1. The corresponding mode shape of the frequency ω_{pj} of the original system is obtained by setting $U_{pj}(x,y)$ in Eq. (30).

2.4 Solution procedure

As an efficient numerical method, the differential quadrature method (DQM) is applied to solve the governing equations of motion obtained in the previous section. Compared to the conventional low order finite difference and finite element methods, the DQ method can result in accurate numerical results by applying a smaller number of grid points; therefore, some computational effort is required (Shu, 2012). However, both the convergency and stability of the solution are intensely dependent upon the distribution of sampling points. Consequently, the well-known Chebyshev nodes are served to discretize the governing equation of motion and the boundary condition expressions, as follows:

$$X_i=\frac{1}{2}\left[1-\cos\left(\frac{i-1}{N-1}\pi\right)\right] \quad i=1,\ 2,\ \cdots,\ N \tag{32}$$

$$Y_i=\frac{1}{2}\left[1-\cos\left(\frac{j-1}{M-1}\pi\right)\right] \quad j=1,\ 2,\ \cdots,\ M \tag{33}$$

In a rectangular plate, a grid of $N\times M$ points is developed. By applying the weighting coefficient, a discretized equation is provided for every point of the grid, to which the following approximation is applied in the governing and boundary equations:

$$\frac{\partial^n f(x_i,y_j)}{\partial x^n}=\sum_{k=1}^{N}\Gamma_{ik}^{(n)}f(x_k,y_j)$$
$$i=1,\ 2,\ \ldots,\ N \quad j=1,\ 2,\ \ldots,\ M \tag{34}$$

$$\frac{\partial^m f(x_i,y_j)}{\partial y^m}=\sum_{k=1}^{M}\bar{\Gamma}_{jk}^{(m)}f(x_i,y_k)$$
$$n=1,\ 2,\ \ldots,\ N-1 \quad m=1,\ 2,\ \ldots,\ M-1 \tag{35}$$

where, N and M are the number of the sampling points in the x and y directions, respectively. $\Gamma_{ik}^{(n)}$ and $\bar{\Gamma}_{jk}^{(m)}$ are the weighting coefficients of the nth derivative of $f(x,y)$ with respect to x and the mth derivative of $f(x,y)$ with respect to y, respectively (Shu, 2012). With the aid of Eqs. (32)–(35), Eq. (23) can be discretized as follows:

$$\sum_{r=1}^{N}\Gamma_{i,r}^{(4)}\bar{U}_{p_{r,j}}+2\lambda^2\sum_{r=1}^{N}\sum_{s=1}^{M}\Gamma_{i,r}^{(2)}\bar{\Gamma}_{j,s}^{(2)}\bar{U}_{p_{r,s}}+$$
$$\lambda^4\sum_{s=1}^{M}\bar{\Gamma}_{j,s}^{(4)}\bar{U}_{p_{i,s}}+\bar{\alpha}_p\bar{U}_{p_{i,j}}+$$
$$\Omega_p^2\left[-\bar{U}_{p_{i,j}}+\frac{\bar{h}^2}{12}\sum_{r=1}^{N}\Gamma_{i,r}^{(2)}\bar{U}_{p_{r,j}}+\lambda^2\frac{\bar{h}^2}{12}\sum_{s=1}^{M}\bar{\Gamma}_{j,s}^{(2)}\bar{U}_{p_{i,s}}\right]=0 \tag{36}$$

A similar approach is applicable to discretize boundary conditions Eqs. (24)–(27) as follows:

$X=0$ (clamped)

$$\bar{U}_{p_{1,j}}=0 \quad \sum_{r=1}^{N}\Gamma_{1,r}^{(1)}\bar{U}_{p_{r,j}}=0 \tag{37}$$

$X = 1$ (Free)

$$\sum_{r=1}^{N} \Gamma_{N,r}^{(2)} \bar{U}_{p_{r,j}} + \upsilon\lambda^2 \sum_{s=1}^{M} \bar{\Gamma}_{j,s}^{(2)} \bar{U}_{p_{N,s}} = 0$$
$$\sum_{r=1}^{N} \Gamma_{N,r}^{(3)} \bar{U}_{p_{r,j}} + (2-\upsilon)\lambda^2 \sum_{r=1}^{N}\sum_{s=1}^{M} \Gamma_{N,r}^{(1)} \bar{\Gamma}_{j,s}^{(2)} \bar{U}_{p_{r,s}} = 0 \quad (38)$$

$Y = 0$ (Free)

$$\lambda^2 \sum_{s=1}^{M} \bar{\Gamma}_{1,s}^{(2)} \bar{U}_{p_{i,s}} + \upsilon \sum_{r=1}^{N} \Gamma_{i,r}^{(2)} \bar{U}_{p_{r,1}} = 0$$
$$\lambda^2 \sum_{s=1}^{M} \bar{\Gamma}_{1,s}^{(3)} \bar{U}_{p_{i,s}} + (2-\upsilon) \sum_{r=1}^{N}\sum_{s=1}^{M} \Gamma_{i,r}^{(2)} \bar{\Gamma}_{1,s}^{(1)} \bar{U}_{p_{r,s}} = 0 \quad (39)$$

$Y = 1$ (Free)

$$\lambda^2 \sum_{s=1}^{M} \bar{\Gamma}_{M,s}^{(2)} \bar{U}_{p_{i,s}} + \upsilon \sum_{r=1}^{N} \Gamma_{i,r}^{(2)} \bar{U}_{p_{r,M}} = 0$$
$$\lambda^2 \sum_{s=1}^{M} \bar{\Gamma}_{M,s}^{(3)} \bar{U}_{p_{i,s}} + (2-\upsilon) \sum_{r=1}^{N}\sum_{s=1}^{M} \Gamma_{i,r}^{(2)} \bar{\Gamma}_{M,s}^{(1)} \bar{U}_{p_{r,s}} = 0 \quad (40)$$

For mixed boundary conditions, the weighting coefficients are combined in a piecewise function (Shu and Wang, 1999). The discretized Eqs. (36)–(40) can be vectorized (Liu and Trenkler, 2008) and assembled in the following form:

$$\begin{cases} \boldsymbol{A}\{U_p\} - \Omega_p^2 \boldsymbol{B}\{U_p\} = 0 \\ \boldsymbol{C}\{U_p\} = 0 \end{cases} \quad (41)$$

where $\{U_p\}$ is the vectorized arrangment of $\bar{U}_{p_{i,j}}$ values. The Eq. (41) is combined by applying the "general approach for implementing boundary conditions" (Shu, 2012) and can be solved by using common matrix algebra.

The lower computational cost of the method proposed for decoupling the equations of motion can be revealed through operations-additions and multiplications required to obtain the natural frequencies, where a determinant should be calculated. Dubbs and Siegel (1987) presented an equation for computing the operations-additions and multiplications required for obtaining an $m \times m$ determinant by way of cofactor expansion expressed as:

$$d = m!\left(1 + \frac{1}{1!} + \frac{1}{2!} + \cdots + \frac{1}{(m-1)!} + \frac{1}{m!}\right) - 2 \quad (42)$$

where d is the total number of operations. By applying the method presented here for decoupling the equations and considering n plates with k sample points for each, it is required to calculate the n determinant of the order k, in which the total operations can be obtained by applying Eq. (42). However, considering all plates simultaneously, one $(n\times k)\times(n\times k)$ determinant should be obtained. If d_1 is assumed as the number of the required operations for the case of decoupling equations and d_2 for the coupled, it is obvious that d_2 is considerably larger than d_1, with the ratio of about $d_2 / d_1 = (n\times k)! / (n\times k!)$. Also, if one applies LU decomposition or the Bareiss algorithm, the elementary operations for an $m\times m$ determinant are of $O(m^3)$ (Shores, 2018). That is, the number of operations for the coupled equations is about n^2 larger than that for the decoupled ones (i.e., $(n\times k)^3 / (n\times k^3) = n^2$). For example, if one considers a triple plate system, i.e., $n = 3$, and applies LU decomposition or the Bareiss algorithm, the number of the required operations for decoupled equations will be about one-ninth of the coupled ones, thereby revealing the computational efficiency of the method introduced in this article.

3 Results and discussions

As a case study for multiple plate systems, a triple plate system is considered with no connection to the ground (i.e., k_1=0 in Eq. (1)), Fig. 3, in which all plates have the same geometry and material properties. A triple plate system can be considered as a development for piezoelectric bimorph plate case studies that frequently have been assessed in the related literature.

To validate the solution method and the precision of its results, rigid connections are considered between the plates ($k_2 \to \infty$ and $k_3 \to \infty$), which makes the triple plate system turn into a system with one plate, allowing a comparison of the frequencies with those presented by Leissa (1973): good agreement is observed therein, as displayed in Table 1.

As for the other case, considering $\lambda = 2$, $\bar{h} = 0.005$, $I_2 = 0$ and $\bar{k}_i = 1048.3$, $i = 1, \ldots, n$, the obtained natural frequencies for elastically connected 3, 5, and 7 plates with an SSSS boundary condition are compared with those presented by Stojanović *et al*. (2015), as shown in Table 2. Excellent agreement is observed, and is therefore a validation of this study. In Table 2, $\bar{k}_i$ is the dimensionless stiffness of the elastic medium between (i-1) th and ith plates, defined as:

$$\bar{k}_i = \frac{a^4}{D} k_i \quad (43)$$

Although the similarity of boundary conditions for all plates is a restriction of the presented method, this situation can be arbitrary. Considering the mixed boundary conditions, a triple plate system is of concern as shown in another case, Fig. 4, in which each plate is simply supported on half of one side and clamped in the other half. In Fig. 4, ξ and η are the lengths of the clamped and simply supported portions, respectively, in which η=2ξ. For $\lambda = 1, \overline{h} = 0.005$ and $\overline{k}_i = 1000$, the first six natural frequencies of the system are tabulated in Table 3 and compared with those obtained by utilizing the ABAQUS finite element software, with which good agreement is observed. The first six mode shapes of the system with those obtained by the ABAQUS software are compared in Fig. 5.

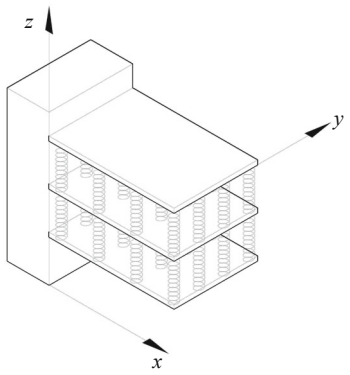

Fig. 3 Elastically connected triple rectangular plates

According to Eq. (23), it is deduced that the vibrational behavior of the system is affected by the factors of geometry and the elastic properties of the connecting medium, represented by Winkler coefficients. The effect of geometry on the vibrational behavior of the system is briefed in the aspect ratio and the dimensionless thickness parameters, Eq. (23). Considering the triple plate system with no connection to the ground, as seen in Fig. 3, the effect of these variables in the dimensionless frequencies is shown in Figs. 6, 7 and 8 for CFFF, CFCF and CCCC boundary conditions, respectively. As observed, the first and second dimensionless frequencies increase for CFFF boundary conditions by an increase in dimensionless thickness with a very small slope, unlike the aspect ratio, in which a decreasing effect is evident. The effect of the aspect ratio on the higher-order frequencies is completely different. In higher-order frequencies, after the third frequency an increase in the aspect ratio would increase dimensionless natural frequencies, as pictured in Fig. 6. For a system with CFCF and CCCC boundary conditions, the dimensionless thickness has a small decreasing effect on dimensionless frequencies, as seen in Figs. 7 and 8, respectively. For special values of λ and $\overline{\alpha}_p$, considering Eq. (23) reveals the dimensionless natural frequency Ω_p that is only affected by the dimensionless thickness, due to terms $(\overline{U}_{p,XX} + \lambda^2 \overline{U}_{p,YY})\,\overline{h}^2/12$. These terms are even neglected in some references due to the slight effects on thin plates (Rao, 2007), leading to the slight effect of

Table 1 Comparison of dimensionless natural frequencies for CFFF boundary conditions ($k_2 \to \infty, k_3 \to \infty, \lambda = 1, \overline{h} = 0.1$)

	Ω_1	Ω_2	Ω_3	Ω_4	Ω_5
Present study	3.4704	8.4704	21.1940	26.9953	30.7213
Leissa (1973)	3.4917	8.5246	21.4290	27.3310	31.1110
Difference (%)	0.61	0.64	1.01	1.23	1.25

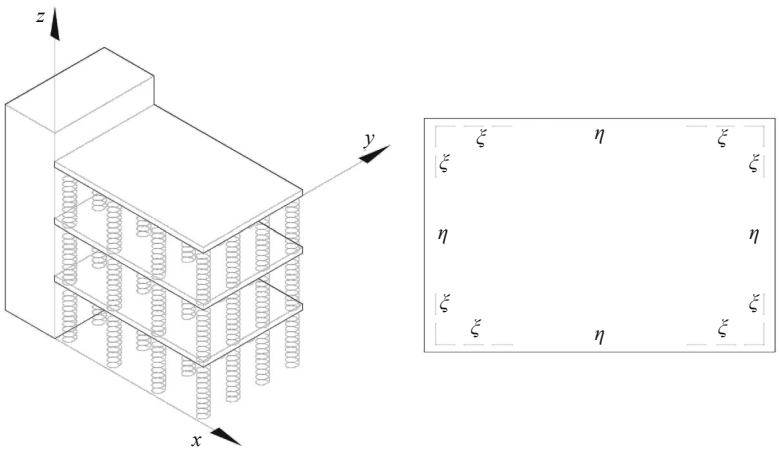

Fig. 4 Triple plate system with mixed boundary conditions (ξ and η, the lengths of the clamped and simply supported portions, respectively)

Table 2 Comparison of natural frequencies (s^{-1}) for SSSS boundary conditions ($\bar{k}_i = 1048.3$, $\lambda = 2$, $\bar{h} = 0.005$, $I_2 = 0$)

Number of plates, n	Frequency number	Present study	Stojanović *et al*. (2015)	Difference (%)
3	1	55.00229	55.00229	0.0
	2	68.21676	68.21676	0.0
	3	81.75544	81.75544	0.0
5	1	53.71028	53.71028	0.0
	2	60.13245	60.13245	0.0
	3	69.61337	69.61337	0.0
	4	78.64206	78.64206	0.0
	5	84.89161	84.89161	0.0
7	1	53.29186	53.29186	0.0
	2	56.97312	56.97312	0.0
	3	63.14726	63.14726	0.0
	4	70.26172	70.26172	0.0
	5	77.00141	77.00141	0.0
	6	82.42263	82.42263	0.0
	7	85.90743	85.90743	0.0

Table 3 The first six natural frequencies (s^{-1}) of the triple plate system, with mixed boundary conditions ($\bar{k}_i = 1000$, $\lambda = 1$, $\bar{h} = 0.005$)

Frequency number	Present study	ABAQUS	Difference (%)
1	10.3339	9.8630	4.6%
2	16.2531	15.646	3.7%
3	20.9051	20.235	3.2%
4	20.9051	20.235	3.2%
5	21.4571	20.521	4.3%
6	24.3803	23.603	3.2%

the dimensionless thickness on dimensionless natural frequencies, as shown in Figs. 6–8. Despite CFFF boundary conditions, all natural frequencies of a system with CCCC boundary conditions increase with a rise in the aspect ratio, Fig. 8. This increase is observed for a system with CFCF boundary conditions except for the first three natural frequencies, in which decreasing the natural frequencies is observed by an increase in the aspect ratio, as shown in Fig. 7. Some numerical results for the first ten dimensionless natural frequencies are tabulated in Tables 4, 5, and 6 for CFFF, CFCF, and CCCC boundary conditions, respectively.

The effects of stiffness coefficients are inquired on in the first fifteen frequencies, as shown in Figs. 9, 10 and 11 for CFFF, CFCF and CCCC boundary conditions, respectively. As anticipated, an increase in the dimensionless frequencies by increasing the stiffness of elastic connections for most frequencies is more evident; that is, increasing stiffness does not affect all

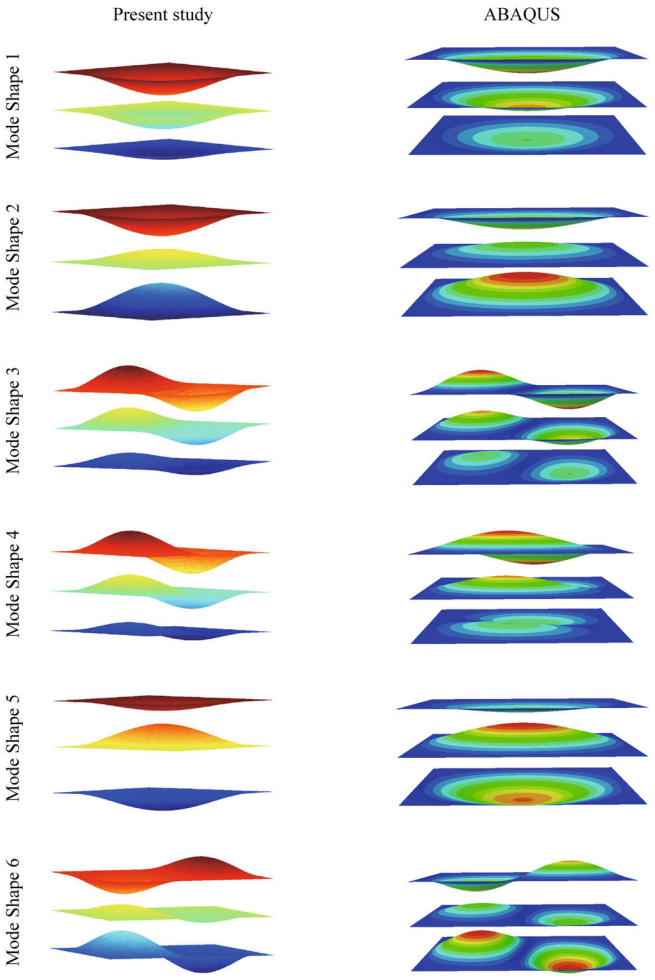

Fig. 5 First six mode shapes of the triple plate system, with mixed boundary conditions ($\bar{k}_i = 1000$, $\lambda = 1$, $\bar{h} = 0.005$)

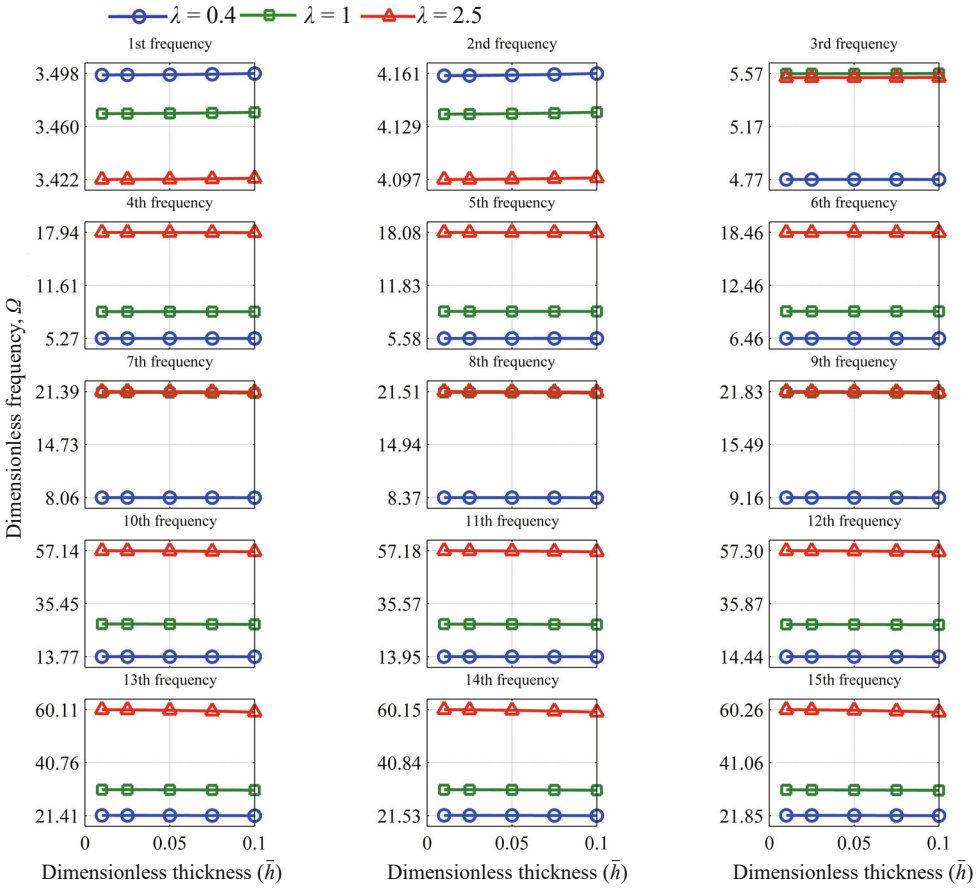

Fig. 6 The effect of dimensionless thickness and aspect ratio on dimensionless natural frequencies ($\bar{k}_2 = 4$, $\bar{k}_3 = 8$, CFFF)

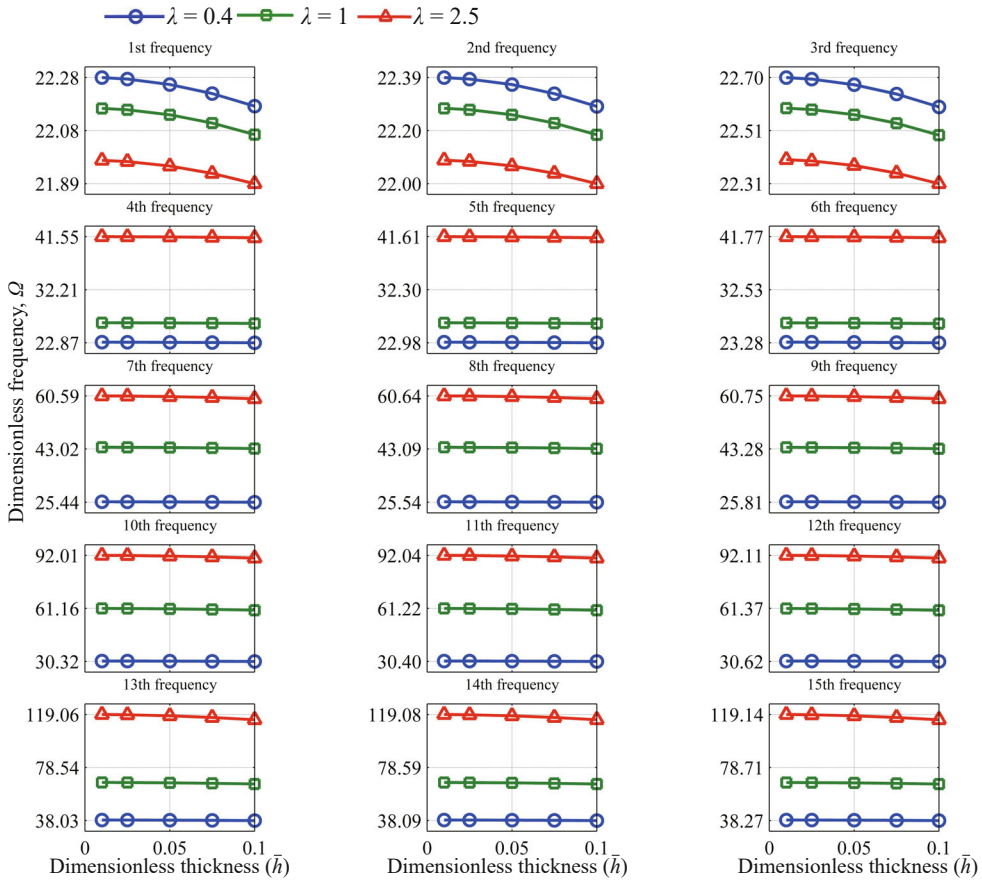

Fig. 7 The effect of dimensionless thickness and aspect ratio on dimensionless natural frequencies ($\bar{k}_2 = 4$, $\bar{k}_3 = 8$, CFCF)

frequencies, but does modify most. On the contrary, with no connection to the ground, the 1st, 4th, 7th, 10th, and 13th dimensionless natural frequencies remain constant, which is due to the identical deflection shape of the similar plates in the corresponding modes, which inactivates the intermediate elastic layers (Ghafarian, and Ariaei, 2016). The first ten dimensionless natural frequencies for different values of stiffness coefficients are tabulated in Tables 7, 8 and 9 for CFFF, CFCF and CCCC boundary conditions, respectively. The

Table 4 The effect of the aspect ratio and dimensionless thickness on the first ten dimensionless natural frequencies ($\bar{k}_2 = 4$, $\bar{k}_3 = 8$, CFFF)

λ	$\bar{h}$	Ω_1	Ω_2	Ω_3	Ω_4	Ω_5	Ω_6	Ω_7	Ω_8	Ω_9	Ω_{10}
0.4	0.01	3.4973	4.1597	4.7700	5.2750	5.5820	6.4561	8.0730	8.3812	9.1707	13.8094
	0.05	3.4975	4.1600	4.7700	5.2749	5.5825	6.4561	8.0709	8.3791	9.1683	13.7995
	0.1	3.4984	4.1610	4.7698	5.2747	5.5838	6.4558	8.0645	8.3724	9.1610	13.7687
1	0.01	3.4694	4.1363	5.5646	8.4748	8.7689	9.5263	21.2829	21.4017	21.7230	27.1598
	0.05	3.4697	4.1366	5.5650	8.4737	8.7678	9.5251	21.2613	21.3799	21.7009	27.1197
	0.1	3.4704	4.1374	5.5661	8.4704	8.7643	9.5213	21.1940	21.3123	21.6322	26.9953
2.5	0.01	3.4220	4.0965	5.5352	17.9367	18.0775	18.4568	21.3889	21.5071	21.8268	57.1391
	0.05	3.4222	4.0968	5.5355	17.9329	18.0737	18.4529	21.3670	21.4851	21.8045	57.0331
	0.1	3.4228	4.0976	5.5365	17.9211	18.0618	18.4407	21.2988	21.4165	21.7349	56.7048

Table 5 The effect of the aspect ratio and dimensionless thickness on the first ten dimensionless natural frequencies ($\bar{k}_2 = 4$, $\bar{k}_3 = 8$, CFCF)

λ	$\bar{h}$	Ω_1	Ω_2	Ω_3	Ω_4	Ω_5	Ω_6	Ω_7	Ω_8	Ω_9	Ω_{10}
0.4	0.01	22.2767	22.3902	22.6975	22.9825	23.0925	23.3906	25.5962	25.6951	25.9633	30.5633
	0.05	22.2513	22.3647	22.6716	22.9559	23.0659	23.3636	25.5589	25.6576	25.9254	30.5026
	0.1	22.1725	22.2855	22.5913	22.8735	22.9831	23.2797	25.4433	25.5415	25.8081	30.3150
1	0.01	22.1642	22.2783	22.5871	26.4002	26.4960	26.7562	43.5860	43.6442	43.8026	61.1593
	0.05	22.1409	22.2549	22.5634	26.3696	26.4653	26.7252	43.4748	43.5328	43.6908	60.9038
	0.1	22.0686	22.1823	22.4897	26.2746	26.3700	26.6289	43.1326	43.1901	43.3469	60.1243
2.5	0.01	21.9748	22.0899	22.4013	41.5476	41.6085	41.7747	60.5937	60.6355	60.7496	92.0102
	0.05	21.9541	22.0691	22.3802	41.5014	41.5623	41.7283	60.3644	60.4060	60.5197	91.6165
	0.1	21.8898	22.0044	22.3147	41.3579	41.4186	41.5840	59.6634	59.7046	59.8170	90.4155

Table 6 The effect of the aspect ratio and dimensionless thickness on the first ten dimensionless natural frequencies ($\bar{k}_2 = 4$, $\bar{k}_3 = 8$, CCCC)

λ	$\bar{h}$	Ω_1	Ω_2	Ω_3	Ω_4	Ω_5	Ω_6	Ω_7	Ω_8	Ω_9	Ω_{10}
0.4	0.01	23.6424	23.7494	24.0393	27.8047	27.8957	28.1429	35.4131	35.4846	35.6793	46.6637
	0.05	23.6092	23.7161	24.0056	27.7515	27.8423	28.0891	35.3160	35.3873	35.5815	46.4828
	0.1	23.5065	23.6129	23.9012	27.5872	27.6775	27.9228	35.0177	35.0884	35.2809	45.9303
1	0.01	35.9816	36.0520	36.2436	73.3764	73.3764	73.4109	73.4109	73.5052	73.5052	108.1762
	0.05	35.8955	35.9657	36.1569	72.9607	72.9607	72.9951	72.9951	73.0888	73.0888	107.2213
	0.1	35.6303	35.7000	35.8898	71.7051	71.7051	71.7388	71.7388	71.8309	71.8309	104.3898
2.5	0.01	147.7196	147.7367	147.7836	173.7062	173.7208	173.7606	221.1986	221.2100	221.2413	291.3998
	0.05	146.4395	146.4565	146.5029	171.6613	171.6757	171.7151	217.4919	217.5031	217.5339	284.5529
	0.1	142.6378	142.6544	142.6996	165.6975	165.7114	165.7494	206.9891	206.9998	207.0291	265.8802

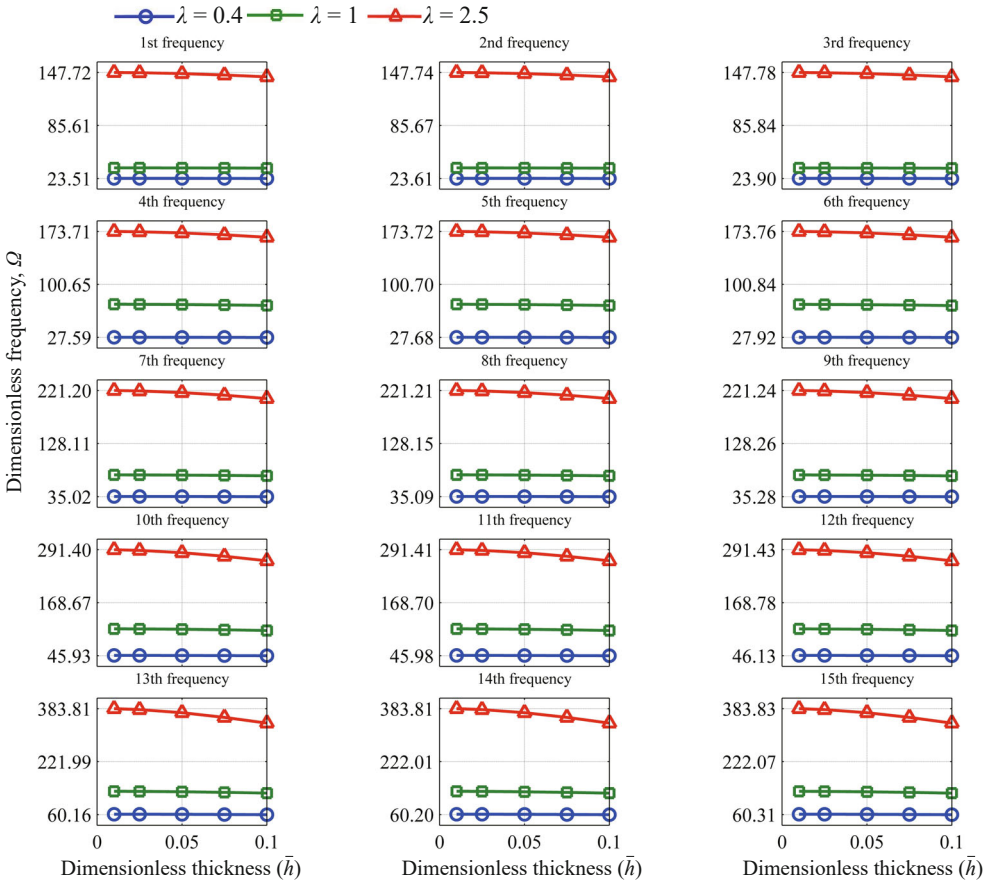

Fig. 8 The effect of dimensionless thickness and aspect ratio on dimensionless natural frequencies ($\bar{k}_2 = 4$, $\bar{k}_3 = 8$, CCCC)

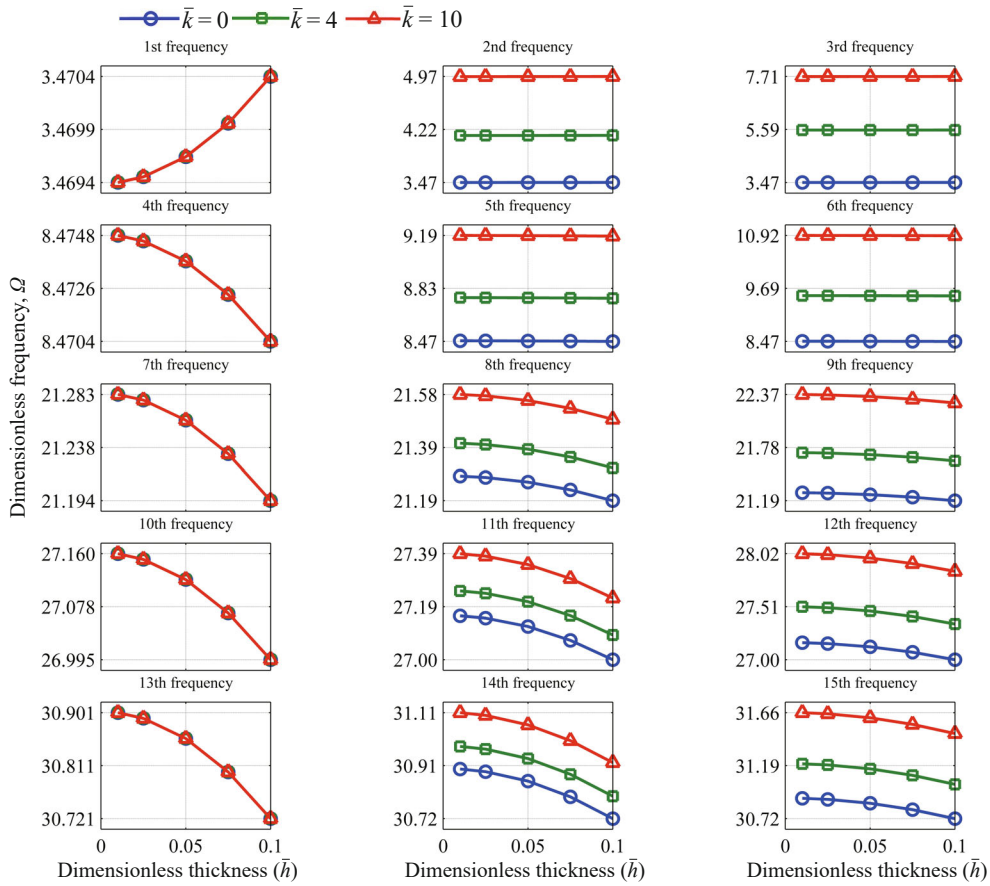

Fig. 9 The effect of stiffness of elastic layers on dimensionless frequencies ($\lambda = 1$, $\bar{k}_2 = \bar{k}$, $\bar{k}_3 = 2\bar{k}$, CFFF)

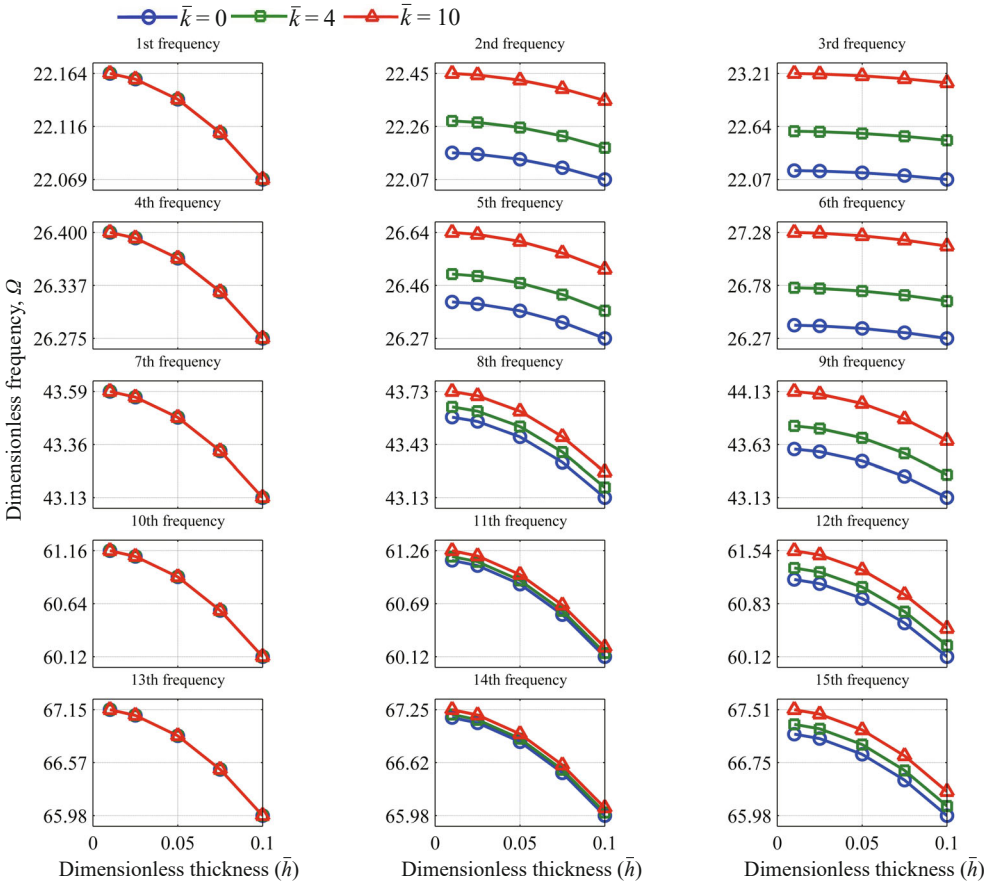

Fig. 10 The effect of stiffness of elastic layers on dimensionless frequencies ($\lambda=1$, $\bar{k}_2=\bar{k}$, $\bar{k}_3=2\bar{k}$, CFCF)

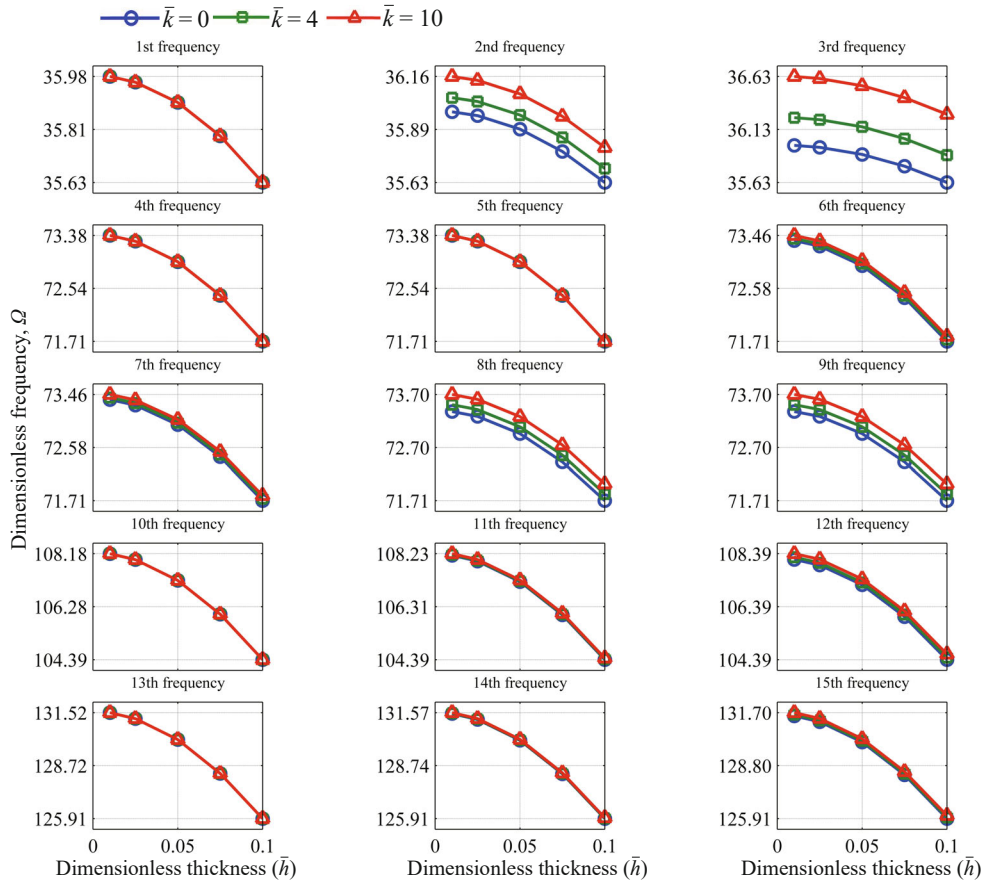

Fig. 11 The effect of stiffness of elastic layers on dimensionless frequencies ($\lambda=1$, $\bar{k}_2=\bar{k}$, $\bar{k}_3=2\bar{k}$, CCCC)

natural frequencies of a system with CCCC boundary conditions exceed those of ones with other boundary conditions followed by CFCF and CFFF plate systems, respectively. This is due to the higher rigidity of a system with clamp boundary conditions, compared to a system with free ones on the same sides. Decreasing the effects of stiffness coefficients in higher-order modes occurs due to an increase in system rigidity.

The stiffness ratio effect on dimensionless frequencies is observed in Fig. 12. The natural frequencies related to modes with the same pattern of plates are not influenced by the ratio between the stiffness coefficients; otherwise, the natural frequencies increase by a rise in k_3. That considering a triple plates system leads to new natural frequencies in the vicinity of natural frequencies of a single plate may present the stiffness ratio as a parameter that could adjust frequencies for some applications such as mechanical energy harvesters (Malaji and Ali, 2017).

The first and the second frequencies of the plates in the decoupled system constitute the first six frequencies of the original system (Ghafarian and Ariaei, 2016). The effect of stiffness coefficients on these frequencies

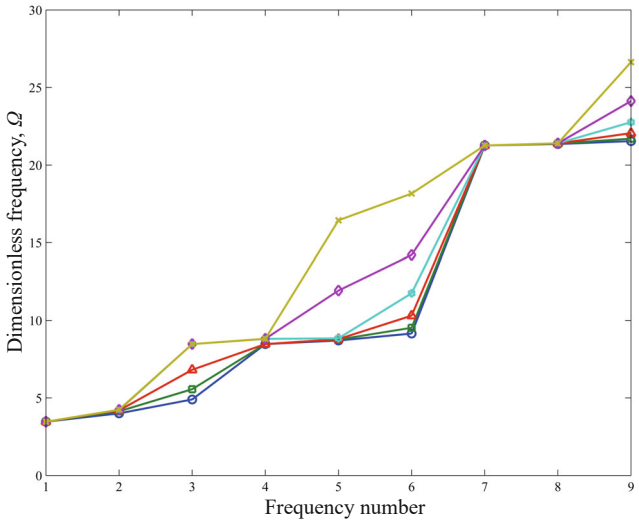

Fig. 12 The effect of the stiffness ratio on dimensionless frequencies (CFFF, $\lambda = 1$, $\bar{h} = 0.05$, $\bar{k}_2 = 4$); $\bar{k}_3 = 4$ (circle), $\bar{k}_3 = 8$ (square), $\bar{k}_3 = 16$ (triangle), $\bar{k}_3 = 32$ (hexagram), $\bar{k}_3 = 64$ (diamond), $\bar{k}_3 = 128$ (cross)

Table 7 The effect of stiffness coefficients on the first ten dimensionless natural frequencies ($\lambda = 1$, $\bar{k}_2 = \bar{k}$, $\bar{k}_3 = 2\bar{k}$, CFFF)

$\bar{k}$	$\bar{h}$	Ω_1	Ω_2	Ω_3	Ω_4	Ω_5	Ω_6	Ω_7	Ω_8	Ω_9	Ω_{10}
0	0.01	3.4694	3.4694	3.4694	8.4748	8.4748	8.4748	21.2829	21.2829	21.2829	27.1598
	0.05	3.4697	3.4697	3.4697	8.4737	8.4737	8.4737	21.2613	21.2613	21.2613	27.1197
	0.1	3.4704	3.4704	3.4704	8.4704	8.4704	8.4704	21.1940	21.1940	21.1940	26.9953
1	0.01	3.4694	3.6476	4.0950	8.4748	8.5493	8.7495	21.2829	21.3127	21.3938	27.1598
	0.05	3.4697	3.6478	4.0953	8.4737	8.5482	8.7484	21.2613	21.2910	21.3720	27.1197
	0.1	3.4704	3.6486	4.0961	8.4704	8.5448	8.7450	21.1940	21.2236	21.3044	26.9953
2	0.01	3.4694	3.8174	4.6369	8.4748	8.6231	9.0159	21.2829	21.3424	21.5041	27.1598
	0.05	3.4697	3.8177	4.6372	8.4737	8.6220	9.0147	21.2613	21.3207	21.4822	27.1197
	0.1	3.4704	3.8185	4.6382	8.4704	8.6186	9.0112	21.1940	21.2532	21.4142	26.9953
4	0.01	3.4694	4.1363	5.5646	8.4748	8.7689	9.5263	21.2829	21.4017	21.7230	27.1598
	0.05	3.4697	4.1366	5.5650	8.4737	8.7678	9.5251	21.2613	21.3799	21.7009	27.1197
	0.1	3.4704	4.1374	5.5661	8.4704	8.7643	9.5213	21.1940	21.3123	21.6322	26.9953
6	0.01	3.4694	4.4322	6.3584	8.4748	8.9123	10.0107	21.2829	21.4609	21.9397	27.1598
	0.05	3.4697	4.4325	6.3588	8.4737	8.9112	10.0094	21.2613	21.4390	21.9174	27.1197
	0.1	3.4704	4.4334	6.3601	8.4704	8.9077	10.0055	21.1940	21.3712	21.8481	26.9953
8	0.01	3.4694	4.7096	7.0635	8.4748	9.0535	10.4727	21.2829	21.5199	22.1543	27.1598
	0.05	3.4697	4.7099	7.0640	8.4737	9.0523	10.4714	21.2613	21.4980	22.1318	27.1197
	0.1	3.4704	4.7109	7.0654	8.4704	9.0488	10.4673	21.1940	21.4299	22.0618	26.9953
10	0.01	3.4694	4.9716	7.7044	8.4748	9.1925	10.9152	21.2829	21.5787	22.3669	27.1598
	0.05	3.4697	4.9719	7.7049	8.4737	9.1913	10.9138	21.2613	21.5568	22.3442	27.1197
	0.1	3.4704	4.9729	7.7065	8.4704	9.1877	10.9095	21.1940	21.4885	22.2734	26.9953

Table 8 The effect of stiffness coefficients on the first ten dimensionless natural frequencies ($\lambda = 1$, $\bar{k}_2 = \bar{k}$, $\bar{k}_3 = 2\bar{k}$, CFCF)

$\bar{k}$	$\bar{h}$	Ω_1	Ω_2	Ω_3	Ω_4	Ω_5	Ω_6	Ω_7	Ω_8	Ω_9	Ω_{10}
0	0.01	22.1642	22.1642	22.1642	26.4002	26.4002	26.4002	43.5860	43.5860	43.5860	61.1593
	0.05	22.1409	22.1409	22.1409	26.3696	26.3696	26.3696	43.4748	43.4748	43.4748	60.9038
	0.1	22.0686	22.0686	22.0686	26.2746	26.2746	26.2746	43.1326	43.1326	43.1326	60.1243
1	0.01	22.1642	22.1928	22.2707	26.4002	26.4242	26.4896	43.5860	43.6006	43.6403	61.1593
	0.05	22.1409	22.1695	22.2473	26.3696	26.3935	26.4589	43.4748	43.4893	43.5289	60.9038
	0.1	22.0686	22.0971	22.1747	26.2746	26.2985	26.3636	43.1326	43.1470	43.1863	60.1243
2	0.01	22.1642	22.2213	22.3767	26.4002	26.4481	26.5788	43.5860	43.6151	43.6944	61.1593
	0.05	22.1409	22.1980	22.3532	26.3696	26.4175	26.5480	43.4748	43.5038	43.5830	60.9038
	0.1	22.0686	22.1255	22.2802	26.2746	26.3223	26.4524	43.1326	43.1614	43.2399	60.1243
4	0.01	22.1642	22.2783	22.5871	26.4002	26.4960	26.7562	43.5860	43.6442	43.8026	61.1593
	0.05	22.1409	22.2549	22.5634	26.3696	26.4653	26.7252	43.4748	43.5328	43.6908	60.9038
	0.1	22.0686	22.1823	22.4897	26.2746	26.3700	26.6289	43.1326	43.1901	43.3469	60.1243
6	0.01	22.1642	22.3352	22.7957	26.4002	26.5438	26.9325	43.5860	43.6732	43.9105	61.1593
	0.05	22.1409	22.3117	22.7717	26.3696	26.5131	26.9013	43.4748	43.5618	43.7984	60.9038
	0.1	22.0686	22.2389	22.6974	26.2746	26.4176	26.8044	43.1326	43.2189	43.4537	60.1243
8	0.01	22.1642	22.3919	23.0023	26.4002	26.5916	27.1076	43.5860	43.7022	44.0181	61.1593
	0.05	22.1409	22.3683	22.9781	26.3696	26.5607	27.0762	43.4748	43.5907	43.9058	60.9038
	0.1	22.0686	22.2953	22.9031	26.2746	26.4651	26.9786	43.1326	43.2476	43.5601	60.1243
10	0.01	22.1642	22.4484	23.2071	26.4002	26.6392	27.2816	43.5860	43.7312	44.1254	61.1593
	0.05	22.1409	22.4248	23.1827	26.3696	26.6083	27.2500	43.4748	43.6196	44.0128	60.9038
	0.1	22.0686	22.3516	23.1070	26.2746	26.5125	27.1518	43.1326	43.2763	43.6664	60.1243

Table 9 The effect of stiffness coefficients on the first ten dimensionless natural frequencies ($\lambda = 1$, $\bar{k}_2 = \bar{k}$, $\bar{k}_3 = 2\bar{k}$, CCCC)

$\bar{k}$	$\bar{h}$	Ω_1	Ω_2	Ω_3	Ω_4	Ω_5	Ω_6	Ω_7	Ω_8	Ω_9	Ω_{10}
0	0.01	35.9816	35.9816	35.9816	73.3764	73.3764	73.3764	73.3764	73.3764	73.3764	108.1762
	0.05	35.8955	35.8955	35.8955	72.9607	72.9607	72.9607	72.9607	72.9607	72.9607	107.2213
	0.1	35.6303	35.6303	35.6303	71.7051	71.7051	71.7051	71.7051	71.7051	71.7051	104.3898
1	0.01	35.9816	35.9992	36.0473	73.3764	73.3764	73.3850	73.3850	73.4086	73.4086	108.1762
	0.05	35.8955	35.9131	35.9610	72.9607	72.9607	72.9693	72.9693	72.9928	72.9928	107.2213
	0.1	35.6303	35.6477	35.6953	71.7051	71.7051	71.7135	71.7135	71.7365	71.7365	104.3898
2	0.01	35.9816	36.0168	36.1128	73.3764	73.3764	73.3936	73.3936	73.4408	73.4408	108.1762
	0.05	35.8955	35.9306	36.0264	72.9607	72.9607	72.9779	72.9779	73.0248	73.0248	107.2213
	0.1	35.6303	35.6652	35.7603	71.7051	71.7051	71.7219	71.7219	71.7680	71.7680	104.3898
4	0.01	35.9816	36.0520	36.2436	73.3764	73.3764	73.4109	73.4109	73.5052	73.5052	108.1762
	0.05	35.8955	35.9657	36.1569	72.9607	72.9607	72.9951	72.9951	73.0888	73.0888	107.2213
	0.1	35.6303	35.7000	35.8898	71.7051	71.7051	71.7388	71.7388	71.8309	71.8309	104.3898
6	0.01	35.9816	36.0871	36.3739	73.3764	73.3764	73.4282	73.4282	73.5695	73.5695	108.1762
	0.05	35.8955	36.0008	36.2869	72.9607	72.9607	73.0123	73.0123	73.1528	73.1528	107.2213
	0.1	35.6303	35.7348	36.0188	71.7051	71.7051	71.7557	71.7557	71.8938	71.8938	104.3898
8	0.01	35.9816	36.1222	36.5037	73.3764	73.3764	73.4454	73.4454	73.6338	73.6338	108.1762
	0.05	35.8955	36.0358	36.4164	72.9607	72.9607	73.0294	73.0294	73.2167	73.2167	107.2213
	0.1	35.6303	35.7696	36.1474	71.7051	71.7051	71.7725	71.7725	71.9566	71.9566	104.3898
10	0.01	35.9816	36.1573	36.6331	73.3764	73.3764	73.4627	73.4627	73.6980	73.6980	108.1762
	0.05	35.8955	36.0708	36.5455	72.9607	72.9607	73.0466	73.0466	73.2805	73.2805	107.2213
	0.1	35.6303	35.8043	36.2755	71.7051	71.7051	71.7894	71.7894	72.0193	72.0193	104.3898

is shown in Fig. 13. The plates are identical, thus, at $k = 0$, the first frequencies of all plates and the second ones coincide, as shown in Fig. 13. As already known, an increase in stiffness coefficients does not affect the first and fourth frequencies due to the similar deflection shape of the plates in the corresponding modes, as shown in Fig. 14, in which the first six modes are illustrated.

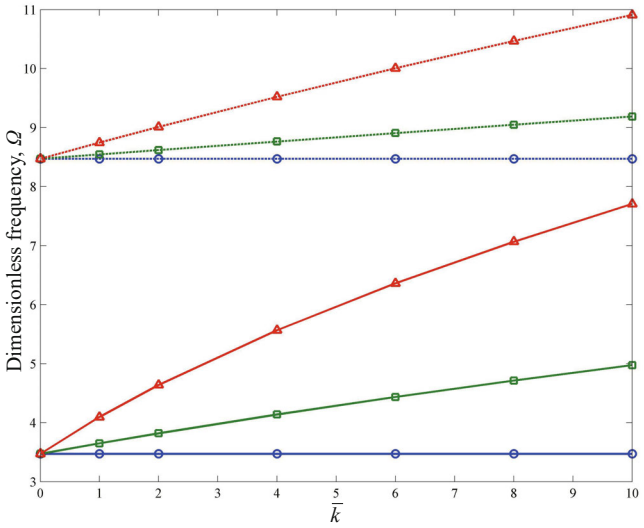

Fig. 13 The effect of stiffness coefficients on the first two frequencies of the decoupled plates ($\lambda = 1$, $\bar{h} = 0.1$, $\bar{k}_2 = \bar{k}$, $\bar{k}_3 = 2\bar{k}$): the decoupled plates' first frequencies (solid-line), the decoupled plates' second frequencies (dash-line); Plate 1 (blue circle), Plate 2 (green square), and Plate 3 (red triangle)

4 Conclusion

The free vibration of an elastically connected multiple plates system is assessed by assuming Kirchhoff's plate theory. Due to difficulties in solving the coupled differential equations, a new change in variables is presented to allow the uncoupling of the equations and to obtain free vibration characteristics by applying the solution methods available for a single plate (such as the differential quadrature method) by means of a reduced computational effort. The two restrictions on this method are (1) the plates must be identical, and (2) the boundary conditions on the same side must be the same, although they can be arbitrary. By assessing the influence of many parameters, the following results are observed:

- As expected, an increase in stiffness coefficients acts to increase most frequencies, while with no connection to the ground due to the similar deflection shape of identical plates in corresponding modes, this does not occur. These frequencies are the same as those of a single plate system.
- The effect of stiffness coefficients in higher-order modes decreases due to an increase in system rigidity.
- The natural frequencies of a system with CFFF boundary conditions, because of the lesser rigidity of the free boundary condition compared to the clamp one, are lower than those of the CFCF and CCCC.
- With no elastic connections, the original and decoupled systems are the same; thus, the natural frequencies of all three plates coincide.
- In a system with thin plates, the effect of the

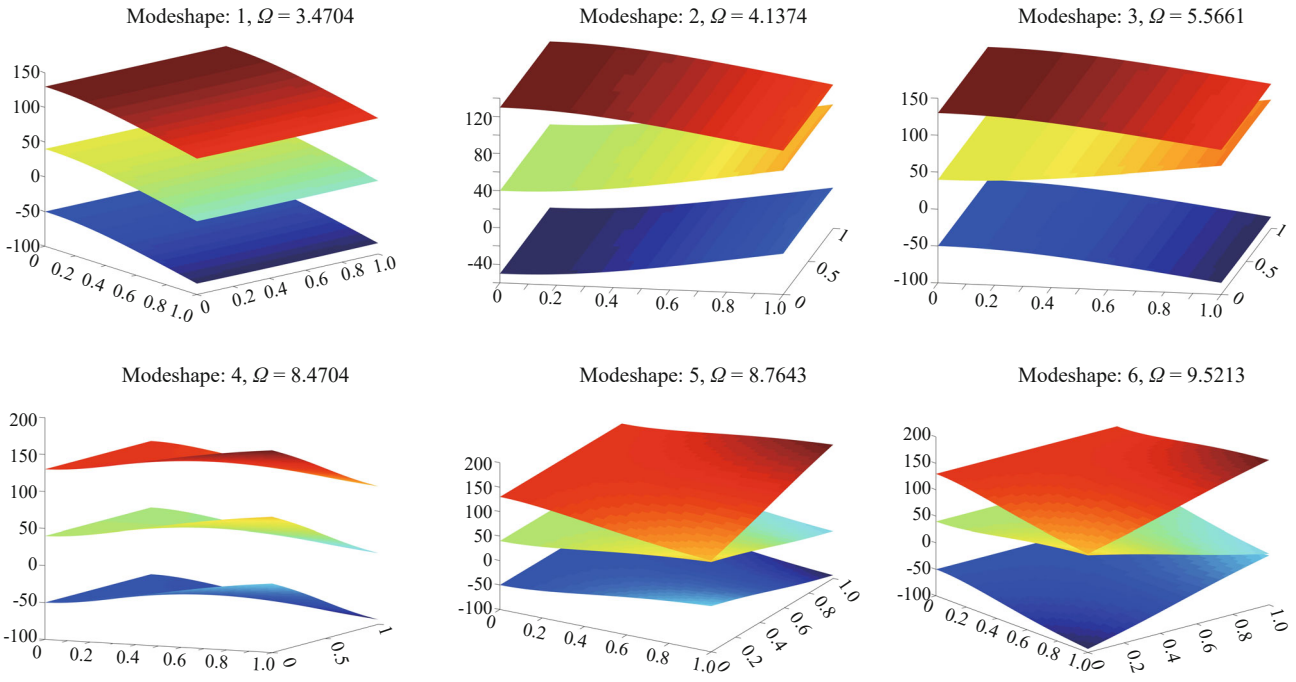

Fig. 14 First six mode shapes of the system ($\lambda = 1$, $\bar{h} = 0.1$, $\bar{k}_2 = 4$, $\bar{k}_3 = 8$)

dimensionless thickness on dimensionless natural frequencies is slight.

- Both the first and second frequencies of a system with CFFF boundary conditions and the first three frequencies for a system with CFCF boundary conditions decrease with an increase in the aspect ratio, while in the case presented here, the effect of the aspect ratio on higher-order frequencies is opposite. All frequencies of a system with CCCC boundary conditions increase, with a rise in the aspect ratio.

This approach can be applied in a system with an arbitrary number of plates with the feature to be modified by considering the various types of mechanical systems, such as parallel membranes and shells.

Acknowledgment

The authors would like to thank the Iran National Science Foundation (INSF) (Grant No. 97021731).

References

Abdel Raheem SE, Abdel Zaher AK and Taha AM (2018), "Finite Element Modeling Assumptions Impact on Seismic Response Demands of MRF-Buildings," *Earthquake Engineering and Engineering Vibration*, **17**(4): 821–834.

Aida T, Kawazoe K and Toda S (1995), "Vibration Control of Plates by Plate-Type Dynamic Vibration Absorbers," *Journal of Vibration and Acoustics*, **117**: 332–338.

Ariaei A, Ziaei-Rad S and Ghayour M (2011), "Transverse Vibration of a Multiple-Timoshenko Beam System with Intermediate Elastic Connections Due to a Moving Load," *Archive of Applied Mechanics*, **81**(3): 263–281.

Arthi S and Jaya K (2020), "Seismic Performance of Precast Shear Wall-Slab Connection Under Cyclic Loading: Experimental Test vs. Numerical Analysis," *Earthquake Engineering and Engineering Vibration*, **19**(3): 739–757.

Bayat M and Pakar I (2013), "Nonlinear Dynamics of Two Degree of Freedom Systems with Linear and Nonlinear Stiffnesses," *Earthquake Engineering and Engineering Vibration*, **12**(3): 411–420.

Bendine K, Boukhoulda FB, Nouari M and Satla Z (2016), "Active Vibration Control of Functionally Graded Beams with Piezoelectric Layers Based on Higher Order Shear Deformation Theory," *Earthquake Engineering and Engineering Vibration*, **15**(4): 611–620.

Bismarck-Nasr MN (1977), "Finite Element Method Applied to the Flutter of Two Parallel Elastically Coupled Flat Plates," *International Journal for Numerical Methods in Engineering*, **11**(7): 1188–1193.

Bochkarev SA and Lekomtsev SV (2016), "Effect of Boundary Conditions on the Hydroelastic Vibrations of Two Parallel Plates," *Solid State Phenomena*, **243**: 51–58.

Brito W, Maia C and Mendonca A (2019), "Bending Analysis of Elastically Connected Euler–Bernoulli Double-Beam System Using the Direct Boundary Element Method," *Applied Mathematical Modelling*, **74**: 387–408.

Busby HR and Weingarten VI (1972), "Non-Linear Response of a Beam to Periodic Loading," *International Journal of Non-Linear Mechanics*, **7**(3): 289–303.

Chonan S (1976), "The Free Vibrations of Elastically Connected Circular Plate Systems with Elastically Restrained Edges and Radial Tensions," *Journal of Sound and Vibration*, **49**(1): 129–136.

Chonan S (1979a), "Elastically Connected Mindlin Plates Subjected to a Moving Load," *Journal of Sound and Vibration*, **63**(3): 452–454.

Chonan S (1979b), "Moving Load on Initially Stressed Thick Plates Attached Together by a Flexible Core," *Ingenieur-Archiv*, **48**(3): 143–154.

Chonan S (1979c), "Resonance Frequencies and Mode Shapes of Elastically Restrained, Prestressed Annular Plates Attached Together by Flexible Cores," *Journal of Sound and Vibration*, **67**(4): 487–500.

Del Carpio M, Hashemi MJ and Mosqueda G (2017), "Evaluation of Integration Methods for Hybrid Simulation of Complex Structural Systems Through Collapse," *Earthquake Engineering and Engineering Vibration*, **16**(4): 745–759.

Duubs C and Siegel D (1987), "Computing Determinants," *The College Mathematics Journal*, **18**(1): 48–50.

Dusicka P, Itani AM and Buckle IG (2004), "Finite Element Investigation of Steel Built-Up Shear Links Subjected to Inelastic Deformations," *Earthquake Engineering and Engineering Vibration*, **3**(2): 195–203.

Ebrahimi F and Heidari E (2019), "Surface Effects on Nonlinear Vibration of Embedded Functionally Graded Nanoplates via Higher Order Shear Deformation Plate Theory," *Mechanics of Advanced Materials and Structures*, **26**(8): 671–699.

Feng YL, Jiang LZ and Zhou WB (2020), "Dynamic Response of a Three-Beam System with Intermediate Elastic Connections Under a Moving Load/Mass-Spring," *Earthquake Engineering and Engineering Vibration*, **19**(2): 377–395.

Foroozandeh S and Ariaei A (2018), "Vibration and Buckling of a Multiple-Timoshenko Beam System Joined by Intermediate Elastic Connections Under Compressive Axial Loading," *Archive of Applied Mechanics*, **88**(7): 1041–1057.

Fu J, Hou Y, Zheng M and Zhu M (2020), "Flexible Piezoelectric Energy Harvester with Extremely High Power Generation Capability by Sandwich Structure

Design Strategy," *ACS Applied Materials and Interfaces*, **12**(8): 9766–9774.

Ghafarian M and Ariaei A (2016), "Free Vibration Analysis of a System of Elastically Interconnected Rotating Tapered Timoshenko Beams Using Differential Transform Method," *International Journal of Mechanical Sciences*, **107**: 93–109.

Giles G (1995), "Equivalent Plate Modeling for Conceptual Design of Aircraft Wing Structures," *Aircraft Engineering, Technology, and Operations Congress*, **95**: 3945.

Gu Q, Liu Y, Li Y and Lin C (2018), "Finite Element Response Sensitivity Analysis of Three-Dimensional Soil-Foundation-Structure Interaction (SFSI) Systems," *Earthquake Engineering and Engineering Vibration*, **17**(3): 555–566.

Hedrih KS (2006), "Transversal Vibrations of Double-Plate Systems," *Acta Mechanica Sinica*, **22**(5): 487–501.

Hedrih KS (2007), "Double Plate System with a Discontinuity in the Elastic Bonding Layer," *Acta Mechanica Sinica*, **23**(2): 221–229.

Hedrih KS (2008), "Energy Transfer in Double Plate System Dynamics," *Acta Mechanica Sinica*, **24**(3): 331–344.

Hedrih KS and Simonović JD (2012), "Multi-Frequency Analysis of the Double Circular Plate System Non-Linear Dynamics," *Nonlinear Dynamics*, **67**(3): 2299–2315.

Irie T, Yamada G and Muramoto Y (1982), "The Axisymmetrical Steady-State Response of Internally Damped Annular Double-Plate Systems," *Journal of Applied Mechanics*, **49**: 417–424.

Jeong KH (2006), "Hydroelastic Vibration of Two Annular Plates Coupled with a Bounded Compressible Fluid," *Journal of Fluids and Structures*, **22**(8): 1079–1096.

Jeong KH and Kang HS (2013), "Free Vibration of Multiple Rectangular Plates Coupled with a Liquid," *International Journal of Mechanical Sciences*, **74**: 161–172.

Jeong KH and Kim JW (2009), "Hydroelastic Vibration Analysis of Two Flexible Rectangular Plates Partially Coupled with a Liquid," *Nuclear Engineering and Technology*, **41**(3): 335–346.

Jouneghani HG and Haghollahi A (2020), "Assessing the Seismic Behavior of Steel Moment Frames Equipped by Elliptical Brace Through Incremental Dynamic Analysis (IDA)," *Earthquake Engineering and Engineering Vibration*, **19**(2): 435–449.

Kamenskikh AO and Lekomtsev SV (2020), "Control of Hydro-Elastic Vibrations of Two Parallel Plates by Electromagnetic Coil," *AIP Conference Proceedings*, **2239**(1): 020020.

Ketiyot R and Hansapinyo C (2018), "Seismic Performance of Interior Precast Concrete Beam-Column Connections with T-Section Steel Inserts Under Cyclic Loading," *Earthquake Engineering and Engineering Vibration*, **17**(2): 355–369.

Khazaee M, Rosendahl L and Rezania A (2020), "A Comprehensive Electromechanically Coupled Model for Non-Uniform Piezoelectric Energy Harvesting Composite Laminates," *Mechanical Systems and Signal Processing*, **145**: 106927.

Kukla S (1998), "Application of Green′s Function in Free Vibration Analysis of a System of Line Connected Rectangular Plates," *Journal of Sound and Vibration*, **217**(1): 1–15.

Kukla S (1999), "Free Vibration of a System of Two Elastically Connected Rectangular Plates," *Journal of Sound and Vibration*, **225**(1): 29–39.

Kunukkasseril VX and Swamidas AJ (1973), "Normal Modes of Elastically Connected Circular Plates," *Journal of Sound and Vibration*, **30**(1): 99–108.

Kunukkasseril VX and Swamidas AJ (1975), "Stability of Continuous Double-Plate Systems," *AIAA Journal*, **13**(10): 1326–1332.

Leissa AW (1973), "The Free Vibration of Rectangular Plates," *Journal of Sound and Vibration*, **31**(3): 257–293.

Li C, Yuan JY, Yu HT and Yuan Y (2018), "Mode-Based Equivalent Multi-Degree-of-Freedom System for One-Dimensional Viscoelastic Response Analysis of Layered Soil Deposit," *Earthquake Engineering and Engineering Vibration*, **17**(1): 103–124.

Li X, Tong G and Zhang L (2020), "Spectra of Seismic Force Reduction Factors of MDOF Systems Normalized by Two Characteristic Periods," *Earthquake Engineering and Engineering Vibration*, **19**(1): 53–69.

Li ZJ and Shu GP (2020), "Test and Evaluation of Modified TADAS Devices with Different Grades of Steel," *Earthquake Engineering and Engineering Vibration*, **19**(2): 451–464.

Liu C, Zheng Z and Yang X (2016), "Analytical and Numerical Studies on the Nonlinear Dynamic Response of Orthotropic Membranes Under Impact Load," *Earthquake Engineering and Engineering Vibration*, **15**(4): 657–672.

Liu FR, Zhang WM, Zhao LC and Zou HX (2020), "Performance Enhancement of Wind Energy Harvester Utilizing Wake Flow Induced by Double Upstream Flat-Plates," *Applied Energy*, **257**: 114034.

Liu S and Trenkler G (2008), "Hadamard, Khatri-Rao, Kronecker and Other Matrix Products," *International Journal of Information and Systems Sciences*, **4**(1): 160–177.

Liu S and Yang B (2019), "A Closed-Form Analytical Solution Method for Vibration Analysis of Elastically Connected Double-Beam Systems," *Composite Structures*, **212**: 598–608.

Liu W, Miao HQ, Wang C and Li J (2020), "Test on a Buried Pipe Network Subjected to an Artificial

Earthquake Produced by Multi-Millisecond Blasting," *Earthquake Engineering and Engineering Vibration*, **19**(3): 791–810.

Lobitz DW, Nayfeh AH and Mook DT (1977), "Non-Linear Analysis of Vibrations of Irregular Plates," *Journal of Sound and Vibration*, **50**(2): 203–217.

Lu J, Peng J, Elgamal A, Yang Z and Law KH (2004), "Parallel Finite Element Modeling of Earthquake Ground Response and Liquefaction," *Earthquake Engineering and Engineering Vibration*, **3**(1): 23–37.

Ma X, Chen K, Ding S, Yu H and Chen J (2014), "Mechanisms of Active Control of Noise Transmission Through Triple-Panel System Using Single Control Force on the Middle Plate," *Applied Acoustics*, **85**: 111–122.

Malaji PV and Ali SF (2017), "Broadband Energy Harvesting with Mechanically Coupled Harvesters," *Sensors and Actuators A*, **255**: 1–9.

Maleki S and Dolati A (2020), "Ductile Steel Plate External End Diaphragms for Steel Tub Girder Straight Highway Bridges," *Earthquake Engineering and Engineering Vibration*, **19**(4): 759–777.

McElman JA (1964), "Flutter of Two Parallel Flat Plates Connected by an Elastic Medium," *AIAA Journal*, **2**(2): 377–379.

Nayfeh AH, Mook DT and Lobitz DW (1974), "Numerical-Perturbation Method for the Nonlinear Analysis of Structural Vibrations," *AIAA Journal*, **12**(9): 1222–1228.

Oniszczuk Z (2000), "Free Transverse Vibrations of an Elastically Connected Rectangular Simply Supported Double-Plate Complex System," *Journal of Sound and Vibration*, **236**(4): 595–608.

Oniszczuk Z (2004), "Forced Transverse Vibrations of an Elastically Connected Complex Rectangular Simply Supported Double-Plate System," *Journal of Sound and Vibration*, **270**(4-5): 997–1011.

Paunović S, Cajić M, Karličić D and Mijalković M (2020), "Dynamics of Fractional-Order Multi-Beam Mass System Excited by Base Motion," *Applied Mathematical Modelling*, **80**: 702–723.

Rao S (2007), *Vibration of Continuous Systems*, John Wiley and Sons, USA.

Reddy JN (2006), *Theory and Analysis of Elastic Plates and Shells*, CRC Press, USA.

Rosa MA and Lippiello M (2009), "Free Vibrations of Simply Supported Double Plate on Two Models of Elastic Soils," *International Journal for Numerical and Analytical Methods in Geomechanics*, **33**(3): 331–353.

Sadri M and Younesian D (2016), "Vibroacoustic Analysis of a Sandwich Panel Coupled with an Enclosure Cavity," *Composite Structures*, **146**: 159–175.

Shores TS (2018), *Applied Linear Algebra and Matrix Analysis*, 2nd ed., Springer, Germany.

Shu C (2012), *Differential Quadrature and Its Application in Engineering*, Singapore: Springer Science and Business Media.

Shu C and Wang CM (1999), "Treatment of Mixed and Nonuniform Boundary Conditions in GDQ Vibration Analysis of Rectangular Plates," *Engineering Structures*, **21**(2): 125–134.

Simonović J (2012), "Non-Linear Dynamics of a Double-Plate System Coupled by a Layer with Viscoelastic and Inertia Properties," *Scientific Technical Review*, **62**(1): 40–54.

Stojanović V, Kozić P and Ristić M (2015), "Vibrations and Stability Analysis of Multiple Rectangular Plates Coupled with Elastic Layers Based on Different Plate Theories," *International Journal of Mechanical Sciences*, **92**: 233–244.

Stojanović V, Petković MD and Deng J (2019), "Stability of Parametric Vibrations of an Isolated Symmetric Cross-Ply Laminated Plate," *Composites Part B: Engineering*, **167**: 631–642.

Swamidas AJ and Kunukkasseril VX (1975), "Free Vibration of Elastically Connected Circular Plate Systems," *Journal of Sound and Vibration*, **39**(2): 229–235.

Swamidas AJ and Kunukkasseril VX (1978), "Vibration of Circular Double-Plate Systems," *The Journal of the Acoustical Society of America*, **63**(6): 1832–1840.

Tahouneh V, Naei MH and Mashhadi MM (2019), "Using IGA and Trimming Approaches for Vibrational Analysis of L-Shape Graphene Sheets via Nonlocal Elasticity Theory," *Steel and Composite Structures*, **33**(5): 717–727.

Tahouneh V, Naei MH and Mashhadi MM (2020), "Influence of Vacancy Defects on Vibration Analysis of Graphene Sheets Applying Isogeometric Method: Molecular and Continuum Approaches," *Steel and Composite Structures*, **34**(2): 261–277.

Tian W, Li Y, Yan Z, Li P and Zhao T (2020), "Suppression of Nonlinear Aeroelastic Responses for a Cantilevered Trapezoidal Plate in Hypersonic Airflow Using an Energy Harvester Enhanced Nonlinear Energy Sink," *International Journal of Mechanical Sciences*, **172**: 105417.

Wang YQ (2018), "Electro-Mechanical Vibration Analysis of Functionally Graded Piezoelectric Porous Plates in the Translation State," *Acta Astronautica*, **143**: 263–271.

Wang YQ, Ye C and Zhu J (2020), "Chebyshev Collocation Technique for Vibration Analysis of Sandwich Cylindrical Shells with Metal Foam Core," *ZAMM Zeitschrift Fur Angewandte Mathematik Und Mechanik*, **100**(5): 1–16.

Wang YQ, Ye C and Zu JW (2019), "Nonlinear Vibration of Metal Foam Cylindrical Shells Reinforced with Graphene Platelets," *Aerospace Science and Technology*, **85**: 359–370.

Wang YQ and Zhao HL (2019), "Free Vibration Analysis of Metal Foam Core Sandwich Beams on Elastic Foundation Using Chebyshev Collocation Method," *Archive of Applied Mechanics*, **89**(11): 2335–2349.

Wang YQ and Zu JW (2017a), "Vibration Behaviors of Functionally Graded Rectangular Plates with Porosities and Moving in Thermal Environment," *Aerospace Science and Technology*, **69**: 550–562.

Wang YQ and Zu JW (2017b), "Analytical Analysis for Vibration of Longitudinally Moving Plate Submerged in Infinite Liquid Domain," *Applied Mathematics and Mechanics* (*English Edition*), **38**(5): 625–646.

Wang YR and Chen SW (2013), "Study of the Positions of Multiple Dampers in a Dual-Plate Mechanism for Vibration Reduction," *Journal of Aeronautics, Astronautics and Aviation A*, **45**(2): 121–134.

Wang YR and Lin TY (2016), "Vibration Reduction of a Double-Layer System Sandwiched with Elastic Medium," *International Journal of Structural Stability and Dynamics*, **16**(10): 1550065.

Wu G and Zhong W (2003), "Mode Analysis of Structures Using the Fourier P-Element Method," *Earthquake Engineering and Engineering Vibration*, **2**(2): 315–318.

Yang FL and Wang YQ (2020), "Free and Forced Vibration of Beams Reinforced by 3 D Graphene Foam," *International Journal of Applied Mechanics*, **12**(5): 2050056.

Yuan TC, Yang J and Chen LQ (2017), "Nonlinear Characteristic of a Circular Composite Plate Energy Harvester: Experiments and Simulations," *Nonlinear Dynamics*, **90**(4): 2495–2506.

Zhang C, Hao H, Kaiming, Bi KM and Yan XY (2020), "Dynamic Amplification Factors for a System with Multiple-Degrees-of-Freedom," *Earthquake Engineering and Engineering Vibration*, **19**(2): 363–375.

Zhao X, Chen B, Li YH, Zhu WD, Nkiegaing FJ and Shao YB (2020), "Forced Vibration Analysis of Timoshenko Double-Beam System Under Compressive Axial Load by Means of Green′s Functions," *Journal of Sound and Vibration*, **464**: 115001.